VIRUS DETECTION WITH DNA LOGIC TAGS

By

Elizabeth Ann Vargis

Thesis

Submitted to the Faculty of the

Graduate School of Vanderbilt University

in partial fulfillment of the requirements

for the degree of

MASTER OF SCIENCE

in

Biomedical Engineering

August, 2007

Nashville, Tennessee

Approved:

Professor F. R. Haselton

Professor David Wright

To Rita Sebastian

ACKNOWLEDGEMENTS

I would like to thank the National Institutes of Health, the Vanderbilt Institute for Integrative Biosystems Research and Education (VIIBRE), and the Vanderbilt University Discovery Grant program for providing the financial resources to complete my research.

This work would not have been possible without the guidance of my two advisors Drs. Rick Haselton and David Wright and the members of their laboratories, especially my co-conspirator Jonas Perez. I am also extremely grateful for the invaluable advice and help of Dr. Kirk Lane, Dr. Susan Opalenik, Chidinma Iwueke, Marcus Gates, Christopher Stowers, and Jerry Wilmink.

Finally, I would like to thank my parents, family members, and friends, particularly those residing on the eighth and ninth floors of Stevenson Center, in the Medical Arts Building, and in Rose Hall.

TABLE OF CONTENTS

LIST OF TABLES

Table Page

LIST OF FIGURES

Figure Page

LIST OF ABBREVIATIONS

Abbreviation	Definition
A, C, G, T, U	Adenine, Cytosine, Guanine, Thymine, Uracil
AuNP	Gold Nanoparticle
bp	base pair
BSA	Bovine Serum Albumin
CCD	Charge-Coupled Device
C_t	Cycle Threshold
DMSO	Dimethylsulfoxide
DTT	Dithiothreitol
ELISA	Enzyme-Linked Immunosorbent Assay
FITC	Fluorescein Isothiocyanate
IPCR	Immuno-Polymerase Chain Reaction
MMP	Magnetic Microparticle
PBS	Phosphate Buffered Saline
PCR	Polymerase Chain Reaction
PFU	Plaque-Forming Unit
QCM	Quartz Crystal Microbalance
RSV	Respiratory Syncytial Virus
SMCC	succinimidyl 4-[N-maleimidomethyl]cyclohexane-1-carboxylate
T_m	Melting Temperature

CHAPTER I

INTRODUCTION

Motivation

An increasing number of molecular biomarkers are used in diagnostic procedures for a wide variety of diseases like influenza, SARS, pneumonia, cancer, and even heart disease. The need for rapid methods to detect low concentrations of biomarkers is becoming more critical. However, current methods of detection often fail when a biomarker is present at low concentrations, potentially leading to situations where a biomarker is not detected (false negative) or a biomarker is incorrectly identified as being present (false positive). Building detection platforms that provide sensitive, reliable, rapid, and quantitative identification of biomarkers would improve the prospects for earlier detection and the timely implementation of the correct course of treatment.

In many detection applications, antibodies are used as the initial detector interface due to their plasticity and very high specificity. Enzyme-linked immunosorbent assays (ELISA) are the gold standard of antibody-based detection technologies.[1] More sensitive methods, like immuno-polymerase chain reactions (IPCR) and antibody-nanoparticle-DNA reporter tag assays have also been developed.[2, 3] However, a drawback of highly sensitive antibody-based detection technologies is the innate presence of non-specific interactions between antibodies and undesired targets, leading to false positives.

The detection platform described in this thesis combines two aspects of previous work, DNA reporter tags and DNA computing, to control for non-specific antibody-

antigen interactions by performing a Boolean NOT operation using nanoparticle surface structures, which we call DNA logic tags. The basic idea of this approach is illustrated in Figure 1 and Figure 2 (Chapter II), which describe the two steps: formation of an ELISA-like antibody-antigen complex (Figure 1) and the implementation of a logical NOT operation (Figure 2).

As shown in Figure 1, a unique DNA logic tag sequence, e.g. A (red line in the upper left), is hybridized to DNA bound to gold nanoparticles. DNA logic tag A is associated with a specific antibody (red branched structure) since they are both conjugated to a gold nanoparticle. Combining this with an antibody-magnetic bead construct, antibody binding to target results in an ELISA-like sandwich and delivery of the DNA tag to an analyte solution. In addition to the gold nanoparticles conjugated to specific antibody and its unique DNA logic tag A (red), a second gold nanoparticle is added to the antigen test solution, which is coupled to a matched non-specific antibody and DNA logic tag A' (green). Although the second antibody is not specific to the target, it may become entrapped non-specifically in the magnetic pulldown complex; this entrapment mirrors any non-specific entrapment of the specific antibody in the magnetic pulldown complex. Sequence A and A' are designed to enable logical operations among tags. In this approach, they can be used to perform tag subtraction to remove non-specific antibody interactions.

Figure 2 describes how the NOT operation is used to subtract non-specific binding events prior to amplification by PCR. DNA logic tag A is designed with a restriction enzyme site and tag A' contains the complementary site. After being released from gold nanoparticles, the tags' complementary regions hybridize. A restriction

enzyme is then used to cleave hybridized A-A'. Figure 2 illustrates the case when tag A is delivered in excess of tag A', which should occur if antibody targets are present in the analyte solution. Restriction enzyme digestion reduces the number of copies of A, but remaining A is amplified by PCR to indicate the presence of target. If the two antibodies are matched with respect to their non-specific binding characteristics, then the reduction in the number of copies of tag A should account for non-specific binding from the specific antibody. This will serve to reduce the likelihood of generating a false positive due to non-specific binding.

In the following pages, traditional, DNA-DNA-based, and antibody-based detection methods are reviewed and tied into recent advances in pathogen detection methods, such as DNA reporter tags. In addition to these topics, DNA computing is also discussed, including Adleman's pioneering work and the latest advances in DNA nanomachines, Boolean control, and logic circuits.

Traditional Methods of Virus Detection

Standard techniques of pathogen detection rely on the growth of the organism in cell culture or replication of virus in a suitable host. While this remains the gold standard for the identification of many viruses, such as respiratory viruses found in nasal secretions, it is an expensive procedure requiring a high level of expertise. Also, the process, which includes purification of the virus prior to testing, can take days to months depending upon what needs to be detected.[4, 5] This application is not practical in situations where accurate results are rapidly needed.[6]

Another way to detect viral products is on the basis of their chemical structures. Traditional analytical chemistry tools, such as gas chromatography-mass spectrometry, can lead to very precise and highly sensitive analyses. However, they are not procedures that can easily be introduced into most laboratories as large and expensive equipment is needed. Also, this method cannot be easily applied to intricate target analytes such as bacteria.[6] These complexities can be solved by identifying specific signature components, but this approach is generally too elaborate for routine and rapid analysis.[7]

Two significant advances have had a profound effect on the speed, specificity, and sensitivity of pathogen detection: (1) recombinant DNA technology, with the development of polymerase chain reaction (PCR) as the key event and (2) methods to generate monoclonal antibodies.[6]

Molecular Recognition Mediated by DNA-DNA Interactions

Any self-replicating biological entity (except prions which do not have nucleic acids associated with them) can be discriminated on the basis of nucleic acid sequences unique to that particular organism.[8] If enough effort has been put into identifying unique sequences that correspond to different viruses, then an assay utilizing nucleic acid-based detection techniques can be used. Sequences are usually determined by chain-termination methods which use PCR with radiolabeled dNTPs and dideoxynucleotides to terminate the replication process. Primers can be developed by replicating fragments of the DNA of interest in bacteria. However, there is a fine line between creating a very specific assay and making assays that are more inclusive to recognize viral variants.[6]

Direct Sequence Detection

One category of nucleic acid-based detection is direct target probing with signal amplification. The basis of these assays is the ability of complementary nucleic acid strands to form stable hybrid complexes. These strands anneal to one another by adhering to Watson-Crick rules of base pairing. The stability of these complexes is highly correlated with the melting temperature (T_m) or the temperature at which half of the hybrid complexes are disassociated. In general, T_m is equivalent to the sum of 2°C for each adenine-thymine (A-T) base pair and 4°C for each guanine-cytosine (G-C) base pair. Other factors also play a role in the stability of the hybrid complex: ionic concentration, pH, length of the complementary sequence, and any mismatches between the strands.[6]

Typically, two probes, complementary to different areas of the target of interest, are designed. One probe is immobilized to a solid support and serves to capture the nucleic acid target. After washing steps are completed, a second probe labeled with a reporter molecule binds to a spatially distinct portion of the target to detect bound target. Since most target nucleic acids are pieces of genomic DNA recovered from biological sources, they are double-stranded and need to be denatured by alkali or heat treatment before hybridization with respective probes.[6]

The reporter can be a variety of molecules, such as radioisotopes, fluorophores, enzymes, or haptens. Radioisotopes were the first molecule utilized within this application, but they are not favored due to their limited half-life, potential toxic effects, and handling concerns.[6] Although directly labeling the immobilized probe with an enzyme or a fluorophore eliminates post-hybridization steps, it can also limit the

performance of a probe due to negative effects on diffusivity and increasing steric hindrance during hybridization. Labeling with haptens and low molecular weight molecules is frequently used to circumvent these issues. One example is biotin-streptavidin: biotin is used to label the probe and a secondary reagent, in this case, a streptavidin-enzyme complex, is added to bind to the biotinylated signal probe to detect the presence of target. Another system uses digoxigenin-labeled probe which binds an anti-digoxigenin antibody-enzyme complex.[6]

Chromogenic substrates are also utilized as reporter molecules. The hydrolysis product is insoluble and can be used for simple visual assays. In general, a color change is observed and scored visually using a spectrophotometer. The main advantage of using colorimetric assays is that the spectrophotometer needed can be small, hand-held, and battery-powered with digital readout and programmable threshold settings to score assays automatically. Sensitivity can be increased by using fluorogenic or chemiluminescent substrates, although they cannot be scored visually and require instrumentation that is not presently available as hand-held models.[6]

Examples of direct sequence detection methods include branched DNA and photolithographically generated oligonucleotide arrays. Branched DNA (Chiron Corporation, Emeryville, CA) uses sequential hybridization of sets of probes resulting in 10^4-fold signal amplification and detection of as low as 10^3 copies of target DNA.[9, 10] GeneChips (Affymetrix, Santa Clara, CA) contain carefully designed and spatially arranged DNA probes in arrays. Fluorescently labeled targets are identified when they hybridize to complementary probes. Fluorescence imagers, like gene array scanners or charge-coupled device (CCD) cameras, are then used to visualize any captured DNA.

Also, detecting nucleic acids by direct hybridization methods has been reported using CCDs, light addressable potiometric sensors, and evanescent wave sensors.[6]

Although the methods discussed above are quite straightforward and simple to perform, they are also time-consuming and require pre-hybridization sample preparation. Furthermore, due to the lack of amplification steps, hybridization-based assays are limited in terms of sensitivity. Most DNA-based systems require at least $10^5 - 10^6$ targets in order to produce a positive result.[6]

Target Amplification

As mentioned above, the need for high concentrations of initial target is a disadvantage of direct sequence detection. This problem can be overcome by amplifying the target which effectively increases the number of targets prior to using one of the detection techniques described above. This additional step has greatly improved direct sequence detection. In fact, a number of post-amplification detection systems have been developed which only rely on initial target amplification.

The development of PCR revolutionized nucleic acid-based diagnostics. By utilizing DNA polymerases that are only active at an increased temperature (for example: *Thermus aquaticus* DNA polymerase), a target region of nucleic acid, defined by a set of oligonucleotide primers, is amplified.[11, 12] One of the key features of PCR is that each newly formed strand becomes a suitable template if the product contains the primer-binding site.[6]

Applying PCR to detection methods has taken many forms. First, if a viral genome is RNA based, direct amplification by PCR can be used if reverse transcription is

first applied to convert RNA to DNA. Second, coupling PCR to any nucleic acid-based detection system results in a significant increase in assay sensitivity. Many of the techniques described above can successfully incorporate PCR as a step prior to detection.

PCR output can be evaluated using a variety of methods. The final product from PCR is detected by agarose or polyacrylamide gel electrophoresis and the addition of an intercalating dye like ethidium bromide or a fluorescent marker that attaches to double-stranded DNA. The result is used to check for molecular weight and to approximate the amount of product formed by measuring the intensity of the band.

A more quantitative approach takes advantage of real-time PCR. This process requires no post-PCR sample handling as the PCR product is evaluated in real-time during the PCR process using a machine that not only cycles through various temperatures, but also contains a light emitter and detector to measure fluorescence.[13] An intercalating dye, like fluorescein, which binds to double-stranded product and measures increases in fluorescence when DNA is replicated, is added to the initial PCR mix. The outcome can then be compared to a standard linear curve to obtain a quantitative result.[14] Newer technologies like TaqMan Probes, which take advantage of the 5' nucleolytic activity of DNA polymerase, release a fluorescent marker every time the probe is incorporated into a newly formed DNA strand, enabling more accurate fluorescence readings.[6]

One disadvantage of this technique is that it remains laboratory-based and requires the services of skilled personnel. While it has been promising initially, it is not extremely rigorous yet and still requires further development in measuring final product with relative certainty.

Ligase chain reactions are similar to PCR, but have been developed to discriminate between targets that differ in only a single base pair. A single base pair difference could mean the difference among the formation of normal, abnormal, and non-functional proteins. Ligation detection reactions are based on the use of two adjacent oligonucleotides designed so that the junction between the 3' end of upstream and downstream primers coincides with the nucleotide that distinguishes one type of target from another.[6, 15] DNA ligase seals the nick between the two oligonucleotides only if the 3' end of one primer is complementary to the target. Therefore, if the two oligonucleotides are ligated, a positive reaction has occurred and the correct target is present. This ligated product can then serve as a template for another round of ligation, leading to a 2-fold increase in the number of templates. While this process is not as robust as PCR, ligase chain reactions are still amplification-based and more specific.[6]

One limitation of both PCR and ligase chain reactions is that they require a thermocycler to quickly change temperatures in order to effect the enzymes involved and allow the reaction to progress.

Molecular Recognition Mediated by Antibody-Based Interactions

Immunological detection uses antibodies to detect any chemical compound that can trigger an immune response. Antibodies to larger molecules like proteins can be made by immunizing an animal with an injection of molecules; antibodies to small molecules that would normally not trigger an immune response are generated by conjugating the smaller molecules to an immunogenic substance before immunizing.

Over time, the antibodies produced by an animal tend to have an increased affinity for the antigen.

Polyclonal and Monoclonal Antibodies

The entire population of antibodies observed in the serum of an immunized animal is termed polyclonal. These antibodies recognize all antigens to which the animal has been exposed to in the past. The specific antigenicity of the compound used to immunize the animal determines how many of the antibodies will be directed against the specific antigen. The main disadvantage of polyclonal antibodies is that they are limited in terms of their specificity due to the presence of cross-reacting antibodies. Sometimes the desired antibodies can be separated by affinity chromatography using an immobilized antigen or by selective absorption of cross-reacting antibodies using an extract prepared from the cross-reactive materials. Another drawback is that polyclonal antibodies are not as abundant as monoclonal antibodies as they are limited to the lifespan of the animal and the amount of serum that can be collected from them. For polyclonal antibodies, antibody-producing cells cannot be directly cultured outside of an animal since they are not transformed and therefore not immortal.[6]

A technological advance in 1975 allowed antibody-producing cells to be grown in culture by fusion with a transformed cell line, granting immortality to the new cell line.[16] Antibody-producing B cells and tumor cells were genetically fused to produce a hybridoma which continues to secrete antibody. Now, individual lines can be cultured as well as selected for by assaying against the desired antigen; this decreases the presence of cross-reacting antibodies.

Enzyme-Linked Immunosorbent Assays

One of the most powerful and most commonly used methods for molecular detection using antibodies is enzyme-linked immunosorbent assays (ELISA). This approach uses enzymes as labels for antibodies. The enzymes are linked to antibodies such that the complexes have both immunological and enzymatic activities. The enzymes degrade chromogenic or fluorogenic substrates, yielding accurate and sensitive detection of the presence of enzyme. First, a polyclonal or monoclonal antibody is adsorbed to the surface of a plate. Then, a solution containing the antigen of interest is added, followed by a series of washing and blocking steps. Next, a different monoclonal antibody labeled with an enzyme is added, followed by the enzyme substrate. The amount of antigen present is correlated to the amount of substrate hydrolyzed, measured by a spectrophotometer or a fluorimeter and compared to a reference negative sample and a standard curve.[1]

One disadvantage of ELISA is that not all antibodies can be used – monoclonal antibodies must be qualified as matched pairs, meaning they must recognize separate epitopes on the antigen so they do not hinder each other's binding. Also, there is a limit to its sensitivity since the amplification is restricted by the amount of enzyme that can be conjugated to antibodies. Immunoreactivity of the antibody may be reduced by enzyme labeling, which in itself is an expensive and time-consuming process.

Recent Advances in Antibody-Based Detection Methods

Current improvements in pathogen detection have attempted to combine the specificity of antibody-based detection methods with the sensitivity of nucleic acid-based amplification procedures. Additionally, in order to increase the sensitivity of detection applications, many nanoscale processes have been developed for the evaluation and recognition of pathogenic particles.

Immuno-Polymerase Chain Reaction

The goal of immuno-polymerase chain reactions (IPCR) is to combine nucleic-acid amplification techniques with conventional antibody-based immunoassays to enhance their sensitivity.[17] In 1992, Sano, *et al*., introduced chimeric conjugates of specific antibodies and nucleic acids in IPCR, with the nucleic acids used as markers to be amplified by standard PCR to generate signal.[2] The advantage of this process is the efficiency from nucleic acid amplification, which can lead to a 100 – 10,000–fold increase in sensitivity, while still maintaining the precision and robustness of the initial antibody-based assay. The more recent development of efficient reagents, the design of assay formats, and the maintenance of functionality, even within complex biological matrices have greatly improved the sensitivity and flexibility of IPCR.[17]

The most prominent obstacle in IPCR is the high background signals that often prohibit meaningful results. Although some noise has been reduced through the use of appropriate blocking protocols, preformed reagents, and optimized antibodies, the problem is still a large limitation of this method.

Antibody-Particle-DNA Reporter Tag Assay

This assay is another powerful detection and amplification system that can be applied to detect nucleic acids and proteins.[3] Two types of particles are used to accomplish sample purification, detection, and amplification. The first is a microparticle with a recognition agent, either an oligonucleotide complementary to the DNA target or a polyclonal antibody. The second is a nanoparticle conjugated to an oligonucleotide complementary to another part of the target DNA or a monoclonal antibody. This nanoparticle also carries hundreds of oligonucleotides referred to as bar-codes, which are 15 - 20-mer oligonucleotides. Once the two particles have sandwiched a target, a magnetic field is used to separate the complexed target and bound nanoparticles from the sample solution. The bar-codes are released by heating the solution or by adding a reducing agent such as dithiothretiol.[18, 19] The bar-codes are then identified with a high sensitivity detection system. Scanometric machines, *in situ* fluorescence-based approaches, and PCR have all been used as the high sensitivity readout mechanism. Although the bio-bar code assay may serve as an alternative to PCR, it may have its most significant impact in protein marker-based diagnostics as it is up to 10^6 times more sensitive than ELISA-based technology.[20]

Again, the major drawback of this application is the possibility for high background signal and the report of false positives due to the use of antibodies as the primary detector.

Antibody-Liposome-PCR

This methodology uses liposomes with encapsulated DNA reporters and ganglioside receptors (non-specific) embedded in the bilayer as a detection agent. The first step of this reaction is similar to ELISA: the target is immobilized by a capture specific antibody. After a blocking step, the liposomal detection reagent is added and allowed to incubate for one hour. After rinsing the plate with phosphate buffered saline (PBS), adding DNase I to degrade unencapsulated DNA, and inactivating it by heat, the liposomes are ruptured with Triton X-100 and the encapsulated reporters are released. The samples are then quantified by real-time PCR with comparison to a standard linear curve.[21]

One of the disadvantages of this approach is that the liposomes with encapsulated reporter sequences do not have a stable shelf-life – the reporter sequences can actually be released from the liposomes over time. Another disadvantage is the possibility for false positives if unencapsulated DNA is not removed completely or if non-specific binding occurs either at the capture antibody or at the non-specific ganglioside level. High background signal can also occur at low concentrations of target due to non-specific binding.

Proximity Ligation Assay

In this technique, the spatial convergence of sets of protein-binding reagents on target molecules brings nucleic acid sequences closer together. After the strands of DNA have been ligated, a DNA reporter sequence is created which can then be amplified. This procedure translates proteins of interest to specific nucleic acid sequences. In general,

sets of target-specific probes are made; these can be antibodies or nucleic acids that have been screened for increased affinity to the target. Each probe has a DNA extension. Once the probes have bound their target, the DNA extensions are brought in proximity to each other. A connector oligonucleotide, added in molar excess, hybridizes to the DNA extensions and guides enzymatic DNA ligation. The ligated DNA sequence is then amplified using real-time PCR and detected. If a probe fails to bind a target molecule, the DNA extensions are not brought together and ligation will not occur.[22-24]

Since this technique relies on antibody or nucleic-acid-based detection, both specificity and sensitivity may be compromised. This problem can especially occur at low concentrations of target.

Filament-Antibody Assay

This approach is based on circumferential bands of antibodies coupled to a 120 μm diameter polyester filament. Automated processing is achieved through sequential positioning of filament-coupled probes through a series of 25 - 60 μl liquid filled microcapillary chambers. Filament motion first positions the antibodies within a microcapillary tube containing a solution of virus before moving the probes through subsequent chambers, where they are washed, exposed to fluorescently labeled antibody, and washed again. A flatbed microarray scanner is used to measure filament fluorescence; an increase in fluorescence can be seen in regions containing antibody-coupled probes. While this design may be useful in point-of-care settings and for the detection of biohazardous materials, its greatest advantage is that it is a tool for automated molecular recognition.[25]

One drawback of this method is the reliance on antibody-based detection, which can lead to false positives, especially with low pathogen concentrations. Also, in its current form, an amplification step is not included, which limits the sensitivity of this technique.

Nanoscale Detection Assays

A variety of nanoscale applications have been recently introduced with the goal of being rapid, sensitive, specific, and economical. For example, atomic force microscopy coupled with an initial immuno-capture step has been used for the direct visualization of viruses by measuring deflections caused by forces or interactions between the tip and surface of the sample. These deflections are measured by a laser beam reflected off a spot on the cantilever at a photodiode detector.[26, 27] Semiconducting nanowires coated with antibodies and configured as field-effect transistors can also be used. When they bind to a charged macromolecule, a change in conductance across the circuit, proportional to the amount of bound target, is detected.[27, 28] Magnetic nanoparticles have also been utilized for their ability to create viral-induced nanoassemblies or agglomerates of viral particles bound by magnetic nanoparticles which can then be visualized by light-scattering experiments.[27, 29] Finally, quantum dots or fluorescent nanoparticles are also being used by looking at two colors that are functionalized with antibodies, spectrally separated, and analyzed for coincidence in real time.[30] One method uses quantum dots conjugated to antibodies to monitor the progression of respiratory syncytial virus (RSV).[31]

The majority of these methods are still quite expensive and, as they are all antibody-based, the possibility of false positives and high background signal remains. Some of them also require complex instrumentation and specialized skills. Finally, these methods are still in the proof-of-concept stage, meaning there is a large amount of optimization needed before they can be used on a wide-scale basis.

DNA and Molecular Computing

As Figure 2 shows, part of our detection method is based on performing logical operations among DNA sequences. For nearly fifteen years, various attempts have been made to manipulate DNA to use it as inputs and outputs of computational operations. The title "DNA computing" is applied to experiments in which DNA molecules have computational roles. Sequences, often about 8-20 base pairs, are used to represent bits and a variety of methods have been devised to manipulate and evaluate them. Certain properties of DNA make it an excellent choice for computational processes – it is both self-complementary (single-stranded DNA selects its own Watson-Crick complement) and it can easily be copied. Also, there is a vast molecular biology toolbox already in place for manipulating DNA, including restriction enzyme digestion, ligation, sequencing, amplification, and fluorescent labeling.[32] Similarly, we propose to use DNA logic tags as inputs to logical operations in our application.

Adleman's Solution to the Traveling Salesman Problem

In his paper in *Science* in 1994, Adleman solved a simplified version of a famous NP-complete computer problem called the Traveling Salesman Problem.[33] NP-complete

problems are a class of search problems for which the correctness of the solution is easy to check. They are also the hardest of problems because they require exponentially increasing amounts of time to solve.[32]

His problem asks whether, given a set of *n* cities ('vertices') with *m* paths ('edges') connecting them, a Hamiltonian path exists that starts at a given vertex v_{in}, passes through each vertex exactly once, and ends at vertex v_{out}. An average computer available today can easily solve this problem for small values of *n*. However, if *n* becomes very large, the amount of time required to generate and check every possible solution increases exponentially, making large calculations very infeasible.[33]

Adleman used a simple, brute-force algorithm which generated random paths through the graphs, discarded any path that did not begin at v_{in} and end at v_{out}, discarded any that did not enter exactly *n* vertices, and discarded any that did not pass through each vertex at least once. He accomplished this by synthesizing a random 20 base pair DNA oligonucleotide to represent each vertex, followed by another series of 20-mers to represent edges.[33] DNA that represented the edge had a certain built-in feature: the first ten nucleotides complemented the last ten bases of one vertex, and the last ten complemented the first ten bases of another vertex. When the mixture of DNA is denatured at high temperatures and then cooled, an oligonucleotide representing an edge will anneal to form a splint to connect both vertices and DNA ligase can join together all possible combinations. The bulk-annealing step allows this molecular approach to test a massive number of possibilities in parallel.[32]

After the first step of denaturing, hybridizing, and ligating, over 10^{13} strands of DNA were generated. Adleman assumed that at least one encoded the Hamiltonian path.

In order to check for this, he used a series of well-developed molecular biology techniques. First, all sequences that began at v_{in} and ended at v_{out} were selectively amplified by PCR using primers specific to those sequences. Any path that did not pass through exactly seven points was eliminated by gel-purifying only the 140-base pair product (equal to seven 20-mers). To remove solutions that did not pass through each vertex exactly once, the product from the gel purification was affinity purified by a single-stranded 20-mer complementary to the sequences of the second vertex. This step was performed for each vertex except the first and last since those were already bound by v_{in} and v_{out} PCR primers.[33]

Any remaining product indicated that a Hamiltonian path did exist. In order to confirm this, graduated PCR was done on the final product, which involved a series of six different PCRs, using the v_{in} forward primer and a primer complementary to each of the other 20-mer vertices, which were then analyzed in separate lanes on a gel. Adleman's path had a readout showing bands of 40, 60, 80, 100, 120, and 140 base pairs.[32]

Comparing this first experimental demonstration of DNA computing to computers of its time, Adleman stated that a typical computer can execute about 10^6 operations per second and the fastest supercomputer can execute about 10^{12}.[33] Although the entire process took about seven days of laboratory work, if each ligation step counts as an operation, Adleman's molecular computer did over 10^{14}. If the ligation step was scaled up, over 10^{20} operations per second could be performed. Also, an extremely small quantity of energy – 2 x 10^{19} ligations (operations) per joule – was consumed, with modern computers operating at 10^9 operations per joule. Finally, one bit of information can be stored in a cubic nanometer of DNA, which is about 10^{12} times more efficient than

existing storage media, meaning that DNA computers have the potential to be faster and more efficient than any electronics developed so far.[32, 33]

At this time, however, DNA computing is still in its infancy. Practical applications have not yet been developed to use on a wide-scale basis.

DNA Nanomachines

Closely related to the performance of logical or computing operations among DNA is the use of DNA to build other structures. Recently, the manipulation of DNA has been extended to DNA nanomachines where DNA is used to build synthetic molecular machinery. It was inspired by biological systems where individual molecules act alone and together as specialized machines. This new technology aims to take advantage of systems already in place within biology. DNA nanomachines are made by self-assembly, using techniques that rely on sequence-specific interactions that bind complementary oligonucleotides together in a double helix. These nanomachines can be activated by interactions with specific signaling molecules or by changes in their environment and can be used for molecular sensing, intelligent drug delivery, or programmable chemical synthesis.[34] Our detection strategy also calls for the use of changes in environment (heat) to create interactions between specific DNA logic tags, enabling their cleavage and the execution of a NOT operation.

Boolean Control and Logic Gates

In 2005, Stojanovic, *et al.*, reported a solution-phase molecular-scale computation media with "Lego-like" deoxyribozyme-based logic gates. Their approach combined the

concept of molecular logic gates with DNA computation and allowed for the bottom-up building of computational complexity in solution. This new application was demonstrated by the synthesis of molecular automata and by the engineering of molecular circuits. They also produced a series of molecules that performed Boolean calculations, allowing for analysis of a series of inputs and a decision process to produce or not produce an output. Output production is based on the presence or absence of inputs and the particular formula they encode. They were also able to use the logic gates to control the functional state of small pieces of oligonucleotides, switching them on or off based on the outcome of previous computations.[35, 36]

Nucleic Acid Logic Circuits

In order to systematically create complex yet reliable circuits, electrical engineers use digital logic, where gates and subcircuits are composed modularly and signal restorations prevent signal degradation. Biological organisms perform complex information processing as well, but engineering synthetic circuits has remained ineffective compared with that of electronic circuits. In 2006, Seelig, *et al.*, reported the design and experimental implementation of DNA-based digital logic circuits, including AND, OR, and NOT gates, signal restoration, amplification, feedback, and cascading. Using single-stranded nucleic acids as inputs and outputs, the mechanism relies solely on sequence recognition and strand displacement.[37]

DNA Logic Tag Computing

Our application describes a new paradigm in DNA log tag antibody-based detection and a practical application of DNA computing embodied within a molecular sensor design. In the proposed approach, DNA logic tags are purposely designed to facilitate logical operations among tags, which are associated to different antibodies. As described in the next chapter, we hypothesize that this approach permits binary NOT operations to control for non-specific antibody interactions among two tags to increase detection specificity without sacrificing sensitivity.

CHAPTER II

VIRUS DETECTION WITH DNA LOGIC TAGS

Abstract

Non-specific antibody binding limits the sensitivity of antibody-based detection technologies. We explore the use of logical operations among DNA logic tags associated with antibodies in order to increase specificity and sensitivity. DNA sequences were developed to perform a logical NOT operation with the goal of subtracting non-specific binding prior to PCR amplification. Antibody-associated tags A and A' are designed to be partially complementary and contain a restriction enzyme site. Tag A is associated with a specific antibody; tag A' is associated with an isotype matched control antibody. If the concentration of A is greater than A', hybridized AA' is enzymatically cleaved and remaining tag A is subsequently amplified during real-time PCR. Quartz crystal microbalance (QCM), DNA agarose gels, and PCR were used to experimentally characterize components of the NOT operation in respiratory syncytial virus (RSV) detection. QCM showed gold nanoparticles functionalized with both tag DNA and antibody bound virus. Successful enzymatic cleavage of AA' was visualized on a DNA agarose gel. After cleavage, remaining tag A was amplified by the addition of primers and standard real-time PCR. In the presence of RSV, magnetic pulldown led to the delivery of both tag A and A'. When PCR was run after enzymatic cleavage, the PCR cycle threshold value was increased. Our results suggest that combining the careful design of DNA logic tags, their association with antibodies, and standard molecular

biology techniques is a promising approach to increase the specificity and sensitivity of antibody-based detection methods.

Introduction

An increasing number of molecular biomarkers are used in diagnostic procedures for a wide variety of diseases like influenza, SARS, pneumonia, cancer, and even heart disease. The need for rapid methods to detect low concentrations of biomarkers is becoming more critical. However, current methods of detection often fail when a biomarker is present at low concentrations, potentially leading to situations where a biomarker is not detected (false negative) or a biomarker is incorrectly identified as being present (false positive). Building detection platforms that provide sensitive, reliable, rapid, and quantitative identification of biomarkers would improve the prospects for earlier detection and the timely implementation of the correct course of treatment.

In many detection applications, antibodies are used as the initial detector interface due to their plasticity and very high specificity. Enzyme-linked immunosorbent assays (ELISA) are the gold standard of antibody-based detection technologies.[1] More sensitive methods, like immuno-polymerase chain reactions (IPCR) and antibody-nanoparticle-DNA reporter tag assays have also been developed.[2, 3] However, a drawback of highly sensitive antibody-based detection technologies is the innate presence of non-specific interactions between antibodies and undesired targets, leading to false positives.

The detection platform described in this thesis combines two aspects of previous work, DNA reporter tags and DNA computing, to control for non-specific antibody-antigen interactions by performing a Boolean NOT operation using nanoparticle surface

structures, which we call DNA logic tags. The basic idea of this approach is illustrated in Figure 1 and Figure 2, which describe the two steps: formation of an ELISA-like antibody-antigen complex (Figure 1) and the implementation of a logical NOT operation (Figure 2).

As shown in Figure 1, a unique DNA logic tag sequence, e.g. A (red line in the upper left), is hybridized to DNA bound to gold nanoparticles. DNA logic tag A is associated with a specific antibody (red branched structure) since they are both conjugated to a gold nanoparticle. Combining this with an antibody-magnetic bead

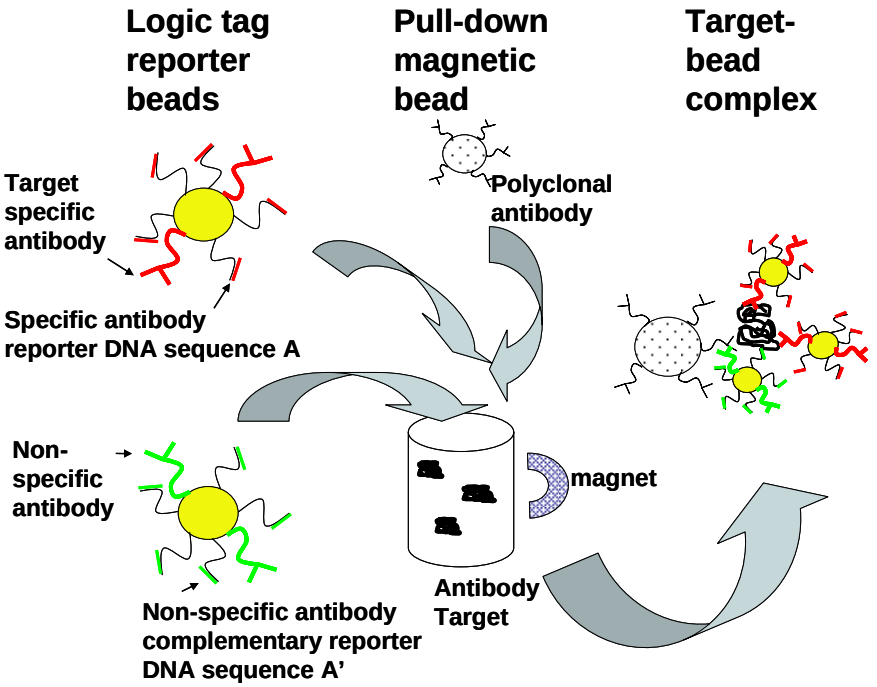

Figure 1. Basic components of the DNA logic tag delivery system. Three components are added to a solution containing antigen: magnetic beads coupled to polyclonal antibody (top center), gold nanoparticles coupled to specific monoclonal antibody and DNA logic tag A (red; top left), and gold nanoparticle coupled to non-specific antibody and logic tag A' (green; bottom left). The presence of antigen in solution results in the magnetic pulldown of the ELISA-like sandwich shown on the right. This complex contains DNA logic tag A associated with specific target antibody and its complement A' associated with non-specific antibody.

construct, antibody binding to target results in an ELISA-like sandwich and delivery of the DNA tag to an analyte solution. In addition to the gold nanoparticles conjugated to specific antibody and its unique DNA logic tag A (red), a second gold nanoparticle is added to the antigen test solution, which is coupled to a matched non-specific antibody and DNA logic tag A' (green). Although the second antibody is not specific to the target, it may become entrapped non-specifically in the magnetic pulldown complex; this entrapment mirrors any non-specific entrapment of the specific antibody in the magnetic pulldown complex. Sequence A and A' are designed to enable logical operations among tags. In this approach, they can be used to perform tag subtraction to remove non-specific antibody interactions.

Figure 2 describes how the NOT operation is used to subtract non-specific binding events prior to amplification by PCR. DNA logic tag A is designed with a restriction enzyme site and tag A' contains the complementary site. After being released from gold nanoparticles, the tags' complementary regions hybridize. A restriction enzyme is then used to cleave hybridized A-A'. Figure 2 illustrates the case when tag A is delivered in excess of tag A', which should occur if antibody targets are present in the

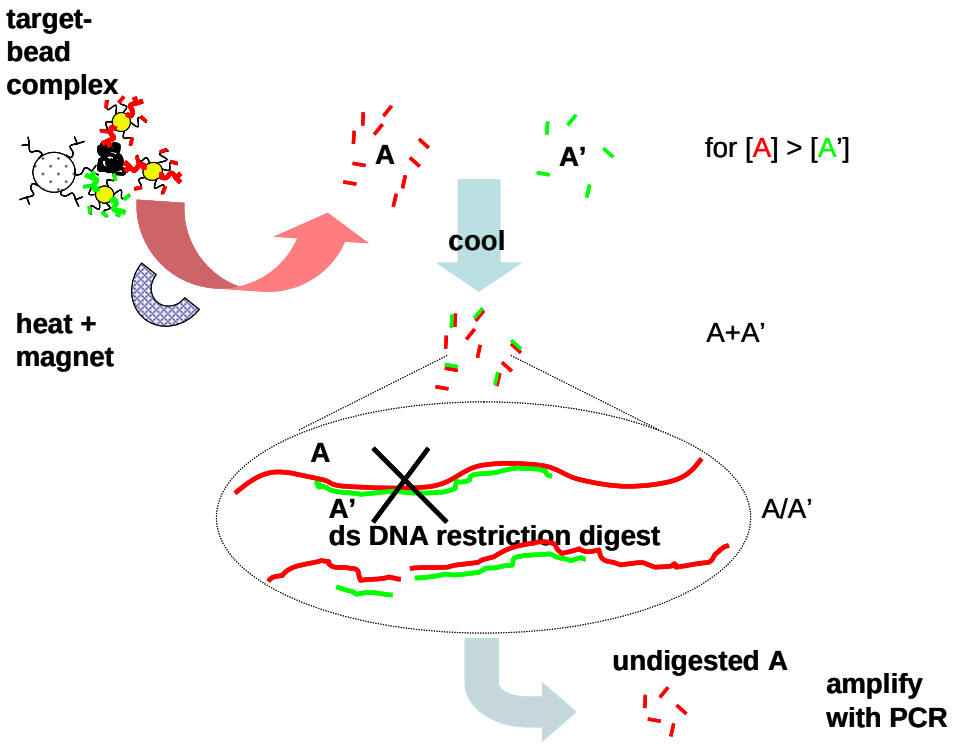

Figure 2. The NOT operation is used to decrease effects of non-specific binding. DNA logic tags are recovered from the sandwich ELISA-like complex by heating. DNA logic tag A contains a restriction enzyme cleavage site. Non-specific antibody interactions deliver complement A'. In the illustration, the presence of antigen results in an excess of tag A compared to tag A'. The hybridized double-stranded DNA (AA') is cleaved by a restriction enzyme. Intact tag A remaining in solution is subsequently amplified and detected by real-time PCR.

analyte solution. Restriction enzyme digestion reduces the number of copies of A, but remaining A is amplified by PCR to indicate the presence of target. If the two antibodies are matched with respect to their non-specific binding characteristics, then the reduction in the number of copies of tag A should account for non-specific binding from the specific antibody. This will serve to reduce the likelihood of generating a false positive due to non-specific binding.

Materials and Methods

DNA Logic Tag Design

Carefully designed DNA structures are critical for the success of this approach. Three criteria were used to design DNA logic tags. First, each oligonucleotide had at least 60 base pairs to make PCR a more reproducible process (since DNA polymerase has an optimal range for amplification) and at most 120 base pairs to allow commercial DNA synthesis. Secondly, the oligonucleotide was designed with a TaqMan® probe site to provide a more specific alternative to intercalating dyes like SYBR Green. Finally, the logic tag sequence was made to contain a blunt-end restriction enzyme cleavage site close to the 3' end. This placement has the largest effect on PCR because DNA replication stops before incorporation of TaqMan probes (Figure 3).

In order to achieve these criteria, initial sequences were generated using two different approaches. First, pieces from the mouse genome found in literature were used as inputs to the applications listed below.[38] Second, sequences from the other parts of the mouse genome were scrambled using an internet-based word scrambler program

(http://www.lerfjhax.com/scrambler) and checked using BLAST to make sure they had little to no similarity with the human genome to decrease the possibility of contamination. Due to the uncertainties associated with the amplification of synthetic DNA, sequences generated both from nature and randomness were input into RealTimeDesign (Biosearch Technologies, Novato, CA) and SciTools Primer Quest (Integrated DNA Technologies, Coralville, IA). In both applications, the TaqMan design model was selected and the initial parameters were set so that the length of the output sequence was between 60 and 120 base pairs. The cleavage site criterion was determined by inputting the oligonucleotide into NEBcutter V2.0 (New England Biolabs, Beverly, MA) to find any blunt-end restriction enzyme site that was 20 to 40 base pairs from the 3' end to avoid the PCR primer site. A restriction enzyme was selected if it reacted with unmethylated DNA strands and if it could be inactivated. Also, it had to have little to no star activity (relaxed or altered specificity) and it should not cleave single-stranded DNA.

If an amplicon, its corresponding primers and TaqMan probe were generated by both programs, it was then selected as a candidate DNA logic tag. The top five assays were selected from both the mouse genome and the word scrambler methods of generating DNA sequences. Ten DNA logic tag candidates in total were chosen, tested, and optimized (see below). They were tested against each other to see how quickly they began to amplify and how few copies could amplify consistently. Each candidate's length was also verified by running the PCR product on an agarose gel (see below). Eight of the ten initial candidates performed well, but most did not consistently amplify lower copy numbers.

From these evaluations, T7-76, a result of the word scrambler method (Figure 3, Table 1), was selected as the best choice to use in subsequent tests. The candidates were labeled sequentially followed by their length, i.e. T7-76 was the seventh candidate tag and it was 76 base pairs long. Every sequence related to T7 began with T7, an abbreviated description (LP = left primer, RP = right primer, comp = complementary strand, RC = restriction complement, TaqMan = TaqMan probe), and its length. T7comp-55 was 40 bases long: an exact complement to the 3' end of T7-76 with a thiol-C6-linker and 15 thymines (Ts) on the 5' end. Fifteen Ts were used as a spacer since they have been shown by others to have the lowest surface interaction with gold to maximize surface coverage and stability.[39]

Figure 3. Schematic of T7-76. This DNA logic tag is 76 bases long and contains sites for primer and TaqMan probe attachment, as well as for specific restriction enzyme cleavage. The white spaces are regions of DNA that do not have a specific purpose besides adding to the length

Restriction Complement Design

To implement the NOT operation, a second sequence closely related to the logic tag was required. This oligonucleotide was complementary to the region surrounding the restriction enzyme site of the DNA logic tag and was random in other regions where logic tag primers could potentially bind. After evaluating the sequence T7-76 with NEBcutter, we found that it had a blunt-end restriction enzyme site for enzyme HpyCh4V

at 44 bases. Accordingly, we designed T7_RC-76 with a 20 base pair region complementary to the restriction digest site; the other 56 bases were generated from the word scrambler program listed above (Table 1). Similar to the complement to T7-76, T7_RCcomp-55 was designed as the exact complement to 40 base pairs of T7_RC-76 with a thiol-C6-linker and 15 Ts.

Table 1. Sequence designs for DNA logic tags 7, 8, and 12. Also shown are the related primers, TaqMan probes, restriction complement (for T7-76 only) and coupling sequences (for T7-76 only).

Sequence Name	Sequence (5' to 3')
T7-76	CTGCGACGATCTACCATCGACGTACCAGGTCGGTTGAAGGA CCGTGCATAGCGAAATCTCAACTTACGAGACAAGC
T7-LP-17	CTGCGACGATCTACCAT
T7-RP-18	GCTTGTCTCGTAAGTTGA
T7-TaqMan	CALFluor® Gold 540CGTACCAGGTCGGTTGAAGGACCBHQ-1
T7comp-55	Thiol-C6-linker-TTTTTTTTTTTTTTTGCTTGTCTCGTAAGTTGAG ATTTCGCTATGCACGGTCCTT
T7_RC-76	TTACGTGGAGTACGCTTTGATTTCGCTATGCACGGTCCCGCA TTTGAGGCCAGTTAGACGGCCAGTTGACCGTACT
T7_RCcomp-55	Thiol-C6-linker-TTTTTTTTTTTTTTTAGTACGGTCAACTGGCCG TCTAACTGGCCTCAAATGCGGG
T8-87	AACGGGAAGCCCATCACCATCTTCCAGGAGCGAGACCCCAC TAACATCAAATGGGGTGAGGCCGGTGCTGAGTATGTCGTGG AGTCT
T8-LP-16	AACGGGAAGCCCATCA
T8-RP-18	AGACTCCACGACATACTC
T8-TaqMan	CAL Fluor® Gold 540CCATCTTCCAGGAGCGAGACCCBHQ-1
T12-96	GGAGAACCCTGGACATTCCAACCCTTCACCTTGGCGAGTCCC TAATCCTCGGCTAACGCAAGGCCAAACCACAATCCTCTTTGG TTGAGTTCCTCG
T12-LP-16	GGAGAACCCTGGACAT
T12-RP-18	CGAGGAACTCAACCAAAG
T12-TaqMan	CAL Fluor® Gold 540CCAACCCTTCACCTTGGCGAGTBHQ-1

Real-Time Polymerase Chain Reaction (PCR): Protocol and Optimization

Real-time PCR was performed using a SmartCycler II thermal cycler system (Cepheid, Sunnyvale, CA). Reactions were done in a 25 µL volume with 12.5 µL of iTaq SYBR Green Supermix with ROX (0.4 mM dATP, 0.4 mM dCTP, 0.4 mM dGTP, 0.8 mM dUTP, iTaq DNA polymerase, 50 units/ml, 6 mM Mg^{+2}, SYBR Green I dye, 1 µM ROX reference dye, and stabilizers, product number 170-8851, Bio-Rad Laboratories, Hercules, CA), 200 nM left and right primers, and nuclease-free water. The best protocol was a three-step PCR, beginning with an initial iTaq DNA polymerase activation step of 95°C for 3 minutes followed by 40 cycles of 95°C for 30 s to denature, 56°C for 30 s to anneal and extend, and 78°C for 6 s to detect fluorescence (see below).

To determine the optimal concentration of primers and $MgCl_2$ as well as the temperature settings and cycle conditions, a variety of optimization steps were completed.[14] The first parameter explored was the concentration of $MgCl_2$. Since iTaq SYBR Green supermix already contains 6 mM Mg^{+2}, additional $MgCl_2$ was added in increments of 25 nmol to bring the final concentration in the PCR mix to 400 nM, 500 nM, 600 nM, 700 nM and 800 nM. For optimization of primer concentration, a similar approach was taken: a range of primer concentrations was tested. First, both the left and right primers were increased in parallel from 100 nM to 500 nM in 100 nM increments. Next, the concentration of one primer was kept constant while the other one varied from 100 nM to 500 nM in 100 nM increments. Finally, the temperature settings were determined by examining the times and temperatures of the annealing and extension steps and the temperature of the read step. The times tested were 15s, 30s, 45s and 60s for the annealing and extension steps. The temperatures of the annealing step were between

52°C and 64°C, incremented by 2°C. For the extension step, temperatures between 60°C and 78°C were tested in increments of 2°C. These results were compared to those from testing combined annealing and extension steps at temperatures between 52°C and 62°C. We were able to take advantage of the Cepheid thermocycler's flexibility and run various reactions in parallel with different temperatures and times for each step in the PCR cycling process.

The optimal parameters for running PCR were determined by evaluating the cycle threshold (C_t) values or the point at which PCR product began to amplify(or pass a certain fluorescence value. Another criteria used to identify the best protocol was if the temperature cycling formed primer dimers; this was determined by melting curve analysis where the product generated by PCR was cooled to 45°C and heated 0.2°C/sec up to 95°C using the thermocycler's melt curve program. The fluorescence was read during the entire process. Primer dimer formation was also verified by agarose gel electrophoresis. Once the optimized protocol and concentrations were determined, they were repeated for verification and used in subsequent reactions.

Decreasing Crossover Contamination

Due to the use of high concentrations of DNA logic tags within our experiments, from PCR, coupling reactions, and restriction digests, steps were taken to minimize the potential for cross-contamination. First, reagents like nuclease free water and primers were aliquotted and new aliquots were typically used daily. Secondly, aerosol barrier tips were always used to decrease accumulation of template within pipettes. Finally, using AmpErase (N808-0096, Applied Biosystems, Foster City, CA) degrades product with

uracil from previous PCR amplifications. Instead of incorporating thymine into our PCR product, the nucleotide mix in the iTaq SYBR Green supermix contained uracil. This provided the option of using AmpErase if PCR product contamination from previous reactions was suspected; in such cases, a preliminary step was added to our standard PCR process of 50°C for 3 minutes before the protocol described above.

Agarose Gel Electrophoresis

To verify the results from PCR and restriction enzyme digestion, agarose gels were run. 10 µL of samples were mixed with 1 µL 10X SYBR Gold (S-11494, Molecular Probes, Eugene, OR) in dimethylsulfoxide (DMSO), and 0.5 µL 10X loading buffer (170-8351, Bio-Rad Laboratories, Hercules, CA). The samples and 5 µL of EZ load 20 base pair molecular ruler (170-8351, Bio-Rad Laboratories, Hercules, CA) combined with 1 µL SYBR Gold were run on a 4% MetaPhor agarose gel (50180, Cambrex Bio Science Rockland, Inc., Rockland, ME) with Tris-Borate-EDTA for 30 minutes to 1 hour at 120 V. The gels were then visualized under 254 nm ultraviolet light using the BioDoc-It Gel Documentation System (UVP, Inc., Upland, CA).

Restriction Enzyme Experiment

To test the NOT operation, T7-76 hybridized with T7_RC-76 were cleaved by the HpyCH4V restriction enzyme which cuts the complementary strands of TG↓CA (5' to 3') and its palindrome AC↓GT (3' to 5'). The reaction was prepared by adding 5 units of HpyCH4V to 88 ng T7-76 and 200 ng T7_RC-76 (corresponding to 5.2×10^{11} and 1.5×10^{12} copies respectively) in incubation buffer (50 mM potassium acetate, 20 mM

Tris-acetate, 10 mM magnesium acetate, 1 mM dithiothreitol, at pH 7.9) from New England Biolabs (R0620S, Beverly, MA). This mixture was then incubated at 37°C for 1 hour, followed by a heat inactivation step of 72°C for 25 minutes. In order to verify the results, the samples were then examined using agarose gel electrophoresis and/or PCR.

Coupling of Antibodies to Magnetic Microparticles

MagnaBind™ amine derivatized 1 μm magnetic microparticles (MMPs, product number 21352, Pierce Biotechnology, Rockford, IL) were activated with succinimidyl 4-[N-maleimidomethyl]cyclohexane-1-carboxylate (SMCC). In a typical reaction, 23 μL of 10 nM SMCC in DMSO were added to 200 μL of MMPs. The solution was mixed and allowed to sit at room temperature for one hour. The MMPs were then cleaned by placing an external magnetic field perpendicular to gravity next to the solution. After one minute, the solution became clear and MMPs were pulled to the side of the tube. When the clear supernatant and the external magnetic field were removed, the MMPs were resuspended in phosphate buffered saline (PBS) at pH 7.4. The washing process was repeated three times.

Antibody reduction was coordinated so that once the MMPs were activated, they could be immediately used. Dithiothreitol (DTT) was used to reduce F-mix antibodies, which is an equal mixture of two anti-respiratory syncytial virus (RSV) fusion protein antibodies (clones 1269 and 1214). 6.1 μL of 1 M DTT was added to 300 μL of purified antibodies at 1 mg/mL concentration in PBS. The solution was mixed and allowed to sit at room temperature for 0.5 hours. After that time, the antibodies were separated from

DTT using a NAP-5 column (17-0853-01, GE Healthcare Bio-Sciences Corp., Piscataway, NJ).

The activated MMPs were combined with the column-purified reduced antibodies and allowed to react for one hour at room temperature. The conjugation was quenched by the addition of β-mercaptoethanol to a final concentration of 100 μM. The remaining solution was purified by placing an external magnetic field perpendicular to gravity next to it. After one minute, the solution became clear and the conjugated MMPs were pulled to the side of the tube. Both the clear supernatant and the external magnetic field were removed; the remaining conjugated MMPs were resuspended in 500 μL PBS. The washing process was repeated three times.

Coupling of Antibodies and DNA to Gold Nanoparticles

Thiolated DNA sequences (T7comp-55, Table 1, Biosearch Technologies, Novato, CA) were received as disulfides and were activated by cleaving the disulfide bond. Cleavage was performed in 100 mM DTT, 0.1 M phosphate buffer, pH 8.3. After 0.5 hours, thiolated DNA was desalted using Microcon YM-3 centrifugal filters (4410, Millipore, Billerica, MA). The purified DNA was diluted to 30 μM in water and stored in small aliquots at -80°C.

In a typical reaction, 3.5 μL of 0.2 mg/mL Synagis® antibody (humanized monoclonal antibody known to target the A antigenic site of RSV's fusion protein, product number NDC 60574-4114-1, MedImmune, Inc., Gaithersburg, MD) were added to 1 mL of 2.325 nM, 15 nm diameter gold nanoparticles (AuNPs, product number 15704-1, Ted Pella, Redding, CA) at pH 9.3 and placed on a rotator for 30 minutes.

After 30 minutes, 20 μL of activated DNA was added; the AuNPs were then rotated for another 30 minutes. The solution was brought to 0.1 M NaCl, 10 mM phosphate buffer, and 0.02% Tween20 and allowed to sit for one hour. After this time, the concentration of NaCl was brought to 0.2 M and to 0.3 M after a third hour. Excess DNA was removed by centrifuging the solution for 30 minutes at 13,200 rpm. The clear supernatant was then removed and the red oily pellet was resuspended in a stock solution of 0.2 M NaCl, 10 mM phosphate buffer, and 0.02% Tween20. This washing process was repeated three times. After washing, particles were resuspended in a stock solution containing DNA logic tags (T7-76, Table 1) and allowed to sit at room temperature overnight. Finally, excess DNA was removed using the washing method described above.

Preparation of RSV stock

RSV stock was prepared by infecting a confluent T-150 flask of HEp-2 cells with RSV. Infection was allowed to proceed for 4 days, after which cells were scraped from the surface of the T-150 flask. The supernatant containing the cells was collected in a 50 mL centrifuge tube. The supernatant was then frozen using a slurry of ethanol and dry ice. After freezing, the supernatant was thawed in a 37°C water bath. The freezing/thawing cycle was repeated three times to ensure the release of virus particles from the cell wall. After the third cycle, the supernatant was separated into aliquots of 1 mL and stored at -80°C.

Titer of Virus Stock

Once the virus stock was prepared, 1 mL aliquots were used to infect 3 columns of a 24-well microtiter plate. After infection, the cells were incubated for 1 hour at 37°C and 5% CO_2. The cells were then overlaid with 1 mL of media containing methylcellulose and incubated for 4 days at 37°C and 5% CO_2. After incubation, the cells were fixed with cold 80% methanol and stored at 4°C for at least one hour. Cells were blocked with 2% BSA in Dulbeccos' PBS (Mg^{2+} and Ca^{2+} free) for 1 hour. After blocking, the cells were incubated for 30 minutes at room temperature with a 1:1000 dilution of F-mix antibody (final concentration of 20 μg/mL). The cells were then washed with PBS and incubated in a 1:1000 dilution of secondary antibody (goat anti-mouse HRP, product number SC-2005, Santa Cruz Biotechnology) for 1 hour. Excess antibody was removed with PBS. The HRP was then developed with a substrate which rendered a colored dot. The dots were then counted to quantify the amount of plaque forming units (PFU) in the aliquots, giving a titer of 4.0×10^5 PFU/mL.

Magnetic Microparticle Pulldown Experiment

Pulldown experiments were performed to validate the attachment of antibodies to magnetic microparticles (MMPs). Ten μL of antibody-conjugated MMPs and 100 μL of a stock solution of RSV (1.675×10^6 PFU/mL) in 2% bovine serum albumin (BSA) were used. MMPs and virus were mixed and placed on a rotator for two hours. Unbound virus was then removed from the MMPs by cleaning as previously described in the antibody-MMP coupling reaction; this was done three times. Next, the MMPs were mixed with 100 μL of 12 μg/mL F-mix antibody with a 655 nm quantum dot attached to the antibody.

The solution was stirred and placed on a rotator for two hours; unbound quantum dot-coupled antibodies were removed by cleaning the beads three times. After cleaning, the MMP-RSV-quantum dot complexes were placed in a 96-well plate on a BioMag® 96-well Plate Side Pull Magnetic Separator (85072, Polysciences, Inc., Warrington, PA) and imaged on a Zeiss Axiovert 200 inverted fluorescence microscope.

Fluorimetric Validation of DNA-Gold Nanoparticle Attachment

Activated DNA was attached to gold nanoparticles following the procedure stated above. After removal of excess activated DNA, complementary DNA with a conjugated fluorescein isothiocyanate (FITC) dye (Operon Biotechnologies, Inc., Huntsville, AL) was added to the AuNPs. As a control, FITC-DNA was also added to PBS without AuNPs. The amount of complementary DNA added to 100 μL of AuNPs or phosphate buffer was varied to determine the optimal molar ratio of DNA:AuNPs for hybridization. After sitting at room temperature for 24 hours, the solution was centrifuged for 30 minutes at 13,200 rpm to pellet the AuNPs and any DNA conjugated to them. Fluorescence of the supernatant was obtained on a Bio-Tek Synergy HT plate reading fluorimeter.

Quartz Crystal Microbalance Validation of Antibody-Gold Nanoparticle Attachment

All quartz crystal microbalance (QCM) experiments were performed on a Maxtek, Inc. Research Quartz Crystal Microbalance with a flow rate of 30 μL/min. The crystals used were 5 MHz Ti/Au quartz crystals. After equilibrating for 30 minutes in PBS, a 5 minute PBS baseline was obtained. A RSV stock solution containing 4.0×10^5

PFU/mL was then allowed to flow over the crystal for 10 minutes, followed by an additional five minutes of PBS. After RSV binding, non-specific binding was blocked by letting a 1% BSA solution flow over the crystal for ten minutes followed by ten minutes of PBS. At this point, the flow was switched to AuNPs functionalized with anti-RSV antibodies and DNA and, as a control, AuNPs functionalized with DNA alone.

Respiratory Syncytial Virus Pulldown with Magnetic Microparticles and Gold Nanoparticles

Pulldown experiments used 5 μL of antibody-conjugated MMPs, 100 μL of a stock solution of RSV ($4.0x10^5$ PFU/mL) or 100 μL of HEp-2 cell lysate as a negative control and 200 μL of 5% bovine serum albumin (BSA). The MMPs, virus, and BSA solution were mixed and placed on a rotator for one hour. Unbound virus was then removed from the MMPs by cleaning as previously described. After being cleaned three times, the MMPs were mixed with 1 μL of 2 nM antibody-DNA functionalized AuNPs and 300 μL of 5% BSA and placed back on the rotator for one hour. The MMPs were then washed two times in 5% BSA followed by three additional washes in PBS. After the final wash, MMPs were resuspended in 200 μL of DNase-free water. Solutions were then held at 90°C for ten minutes followed by placement in an external magnetic field and removal of 150 μL of supernatant. The supernatant was then used in PCR and restriction cleavage reactions.

Results

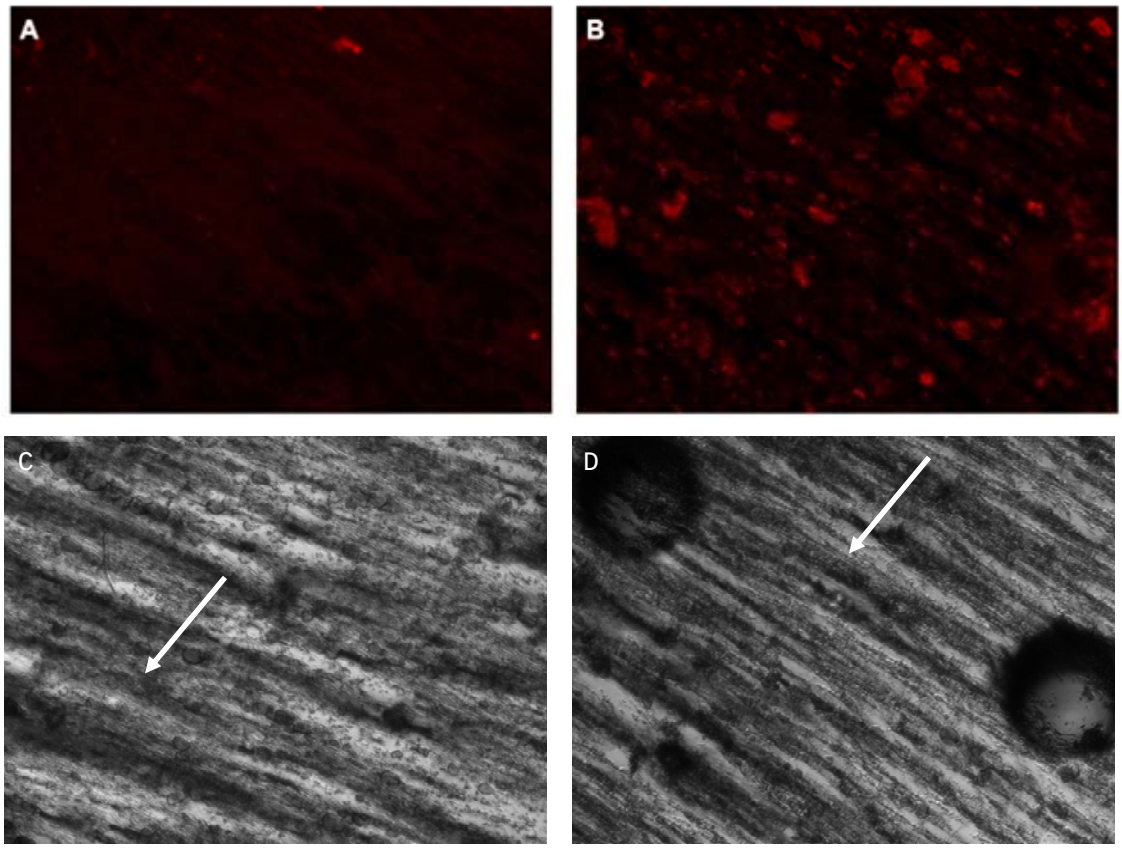

Figure 4. Images of antibody-virus complexes after magnetic pulldown experiments in RSV. A mixture of MMPs unconjugated (left panels) or conjugated (right panels) to F-mix antibodies and 655 nm quantum dots conjugated to F-mix antibodies were mixed with RSV. Magnetic particles and associated complexes were extracted and washed. A&C: Fluorescence and DIC images of unconjugated MMPs; B&D: Fluorescence and DIC images of MMPs conjugated to F-mix antibodies. The striated patterns in the DIC images are thought to be due to the accumulation of MMPs along magnetic field lines (white arrows). All images 20x (unpublished, Perez, *et al.*).

A magnetic pulldown experiment shows that antibodies remain functional after attachment to MMPs (Figure 4). After F-mix antibody conjugated MMPs were mixed with RSV, magnetic pulldown was used to extract bound virus. Bound RSV was visualized by the addition of a fluorescent 655 nm quantum dot also attached to F-mix

antibodies. Unbound quantum dot was removed by applying a magnetic field and washing. In panel B, the fluorescence spots are due to the presence of the fluorescent quantum dot within the MMP-RSV complexes. As a control, MMPs not conjugated to F-mix antibody were also exposed to RSV, followed by the pulldown and addition of quantum dots. Panel A shows the fluorescence image from this experiment which contains almost no fluorescence. In panels C and D, the DIC images both show striations due to the MMPs lining up when a magnetic field is applied in the bottom right corner of both images. The two large black spots in panel D are due to air bubbles.

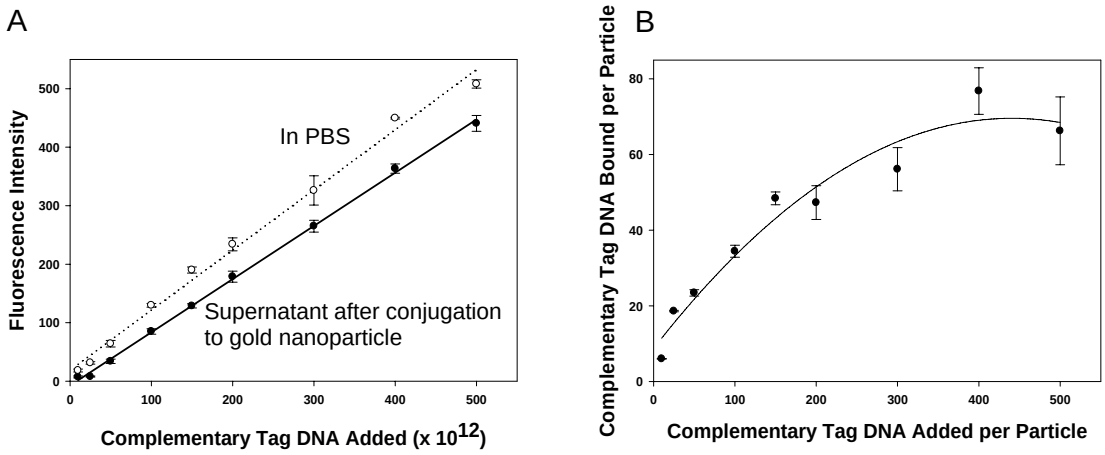

Figure 5. The maximum number of complementary thiolated DNA strands associated with each gold nanoparticle was determined using the methods illustrated in this figure. A. An increased concentration of FITC-labeled DNA logic tags coupled to gold nanoparticles (——) resulted in a difference in fluorescence intensity of the supernatant compared to FITC-labeled DNA alone (. . . .). B: Number of strands bound per particle versus number of strands added per particle (unpublished data, Perez, *et al.*).

The maximum number of thiolated DNA strands (complementary to DNA logic tags) bound to a 15 nm diameter gold nanoparticle was found to be about 70 (Figure 5). Panel A shows the fluorescence measurement from the supernatant after FITC-labeled

DNA is salt-aged with gold nanoparticles and the particles are spun out of solution. For any given thiolated DNA concentration, the fluorescence is decreased in comparison to the same amount of DNA added to PBS alone. The reduction in fluorescence suggests that DNA has attached to the gold nanoparticles. Subtracting the amount of DNA found in the supernatant from what was originally added (from the fluorimeter readings) led to an estimation of the amount of DNA bound to particles (Panel B). At low concentrations of DNA (less than 200 strands per particle), the number of tags per particle increases linearly with increases in initial DNA concentration. Above ~200 strands, addition to the gold nanoparticles becomes non-linear and saturated, eventually reaching a plateau.

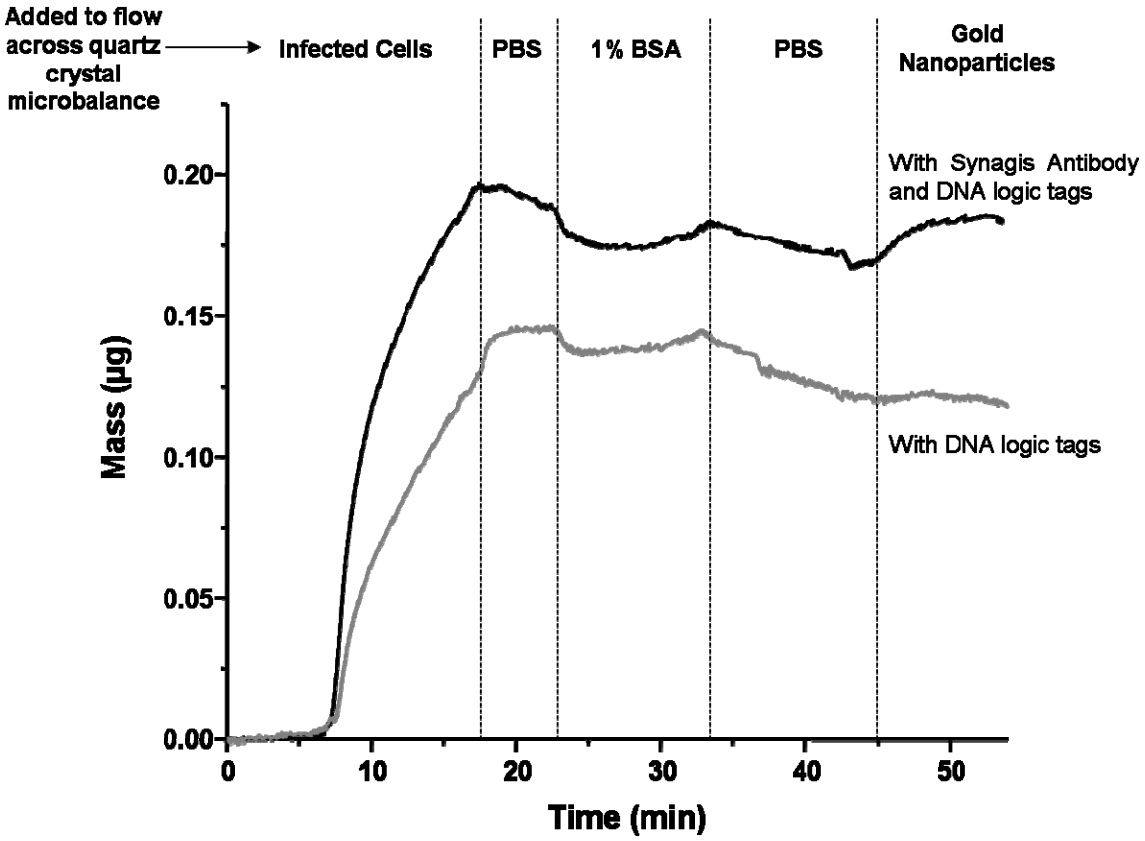

Figure 6. Time course of mass changes when balance-associated RSV was exposed to gold nanoparticles coupled to either DNA logic tags alone (grey line) or to DNA logic tags + Synagis (anti-RSV) antibody (black line). RSV was flowed onto the quartz crystal, followed by a PBS wash. Non-specific binding was blocked with 1% BSA. After excess BSA was washed with PBS, gold nanoparticles coupled to DNA logic tags and Synagis antibody were flowed onto the quartz crystal (black line). Gold nanoparticles with DNA logic tags and no antibody served as a control (grey line, unpublished data, Perez, *et al.*)

Gold nanoparticles conjugated to anti-RSV antibodies and DNA logic tags have a greater affinity for RSV than gold nanoparticles conjugated to DNA alone (Figure 6). In this experiment, RSV was bound via hydrophobic interactions to the crystal on a microbalance. This was followed by washing and blocking steps. Gold nanoparticles with antibodies and DNA were then flowed along the crystal and along any bound RSV. Changes in mass alter the vibration of the crystal; these changes were measured using a

quartz crystal microbalance. By comparing the addition of gold nanoparticles conjugated to antibodies and DNA to the addition of gold nanoparticles with DNA only, an increase in mass of about 0.03 μg was observed. One 15 nm gold nanoparticle with a density of 19,300 kg/m^3 weighs ~3.4×10^{-11} μg. Assuming that gold nanoparticles make up the majority of the weight of the gold nanoparticle-antibody-DNA complex, an increase of 0.03 μg is equivalent to almost 900 million nanoparticles remaining on the crystal. This suggests that the anti-RSV antibodies coupled to the gold nanoparticles are adhering to the RSV found on the crystal. Also, gold nanoparticles with DNA alone do not seem to have much non-specific binding to RSV or BSA since an increase in mass is not seen.

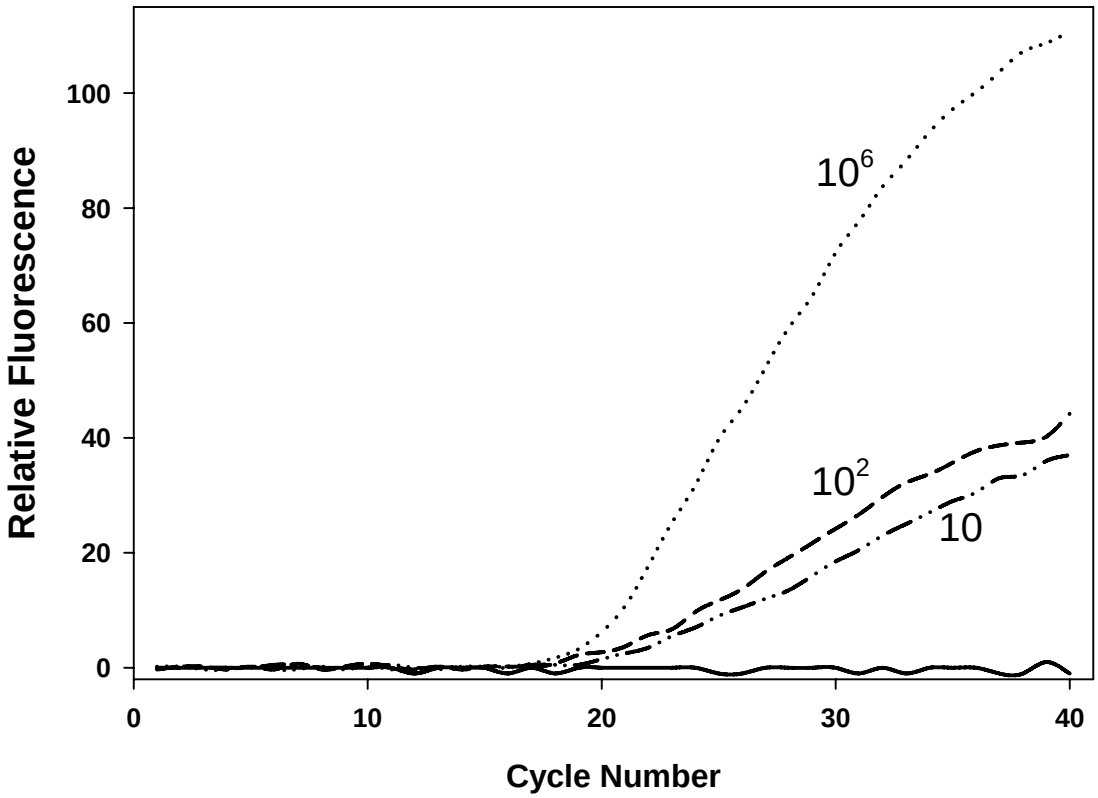

Figure 7. Results of a typical real-time PCR experiment for a range of initial copy numbers of DNA logic tag T7-76. 10^6 copies (....) of initial template begin to amplify first and have a cycle threshold (C_t) value of 18.5 cycles ± 0.71 (mean ± s.d., n = 2); lower concentrations had lower C_t values (100 = 20.5 cycles ± 2.12 (– – –, n = 2), 10 = 21.5 cycles ± 0.71 (— ·, n = 2)). The control with no initial template (——) does not reach the fluorescence level to generate a C_t value (n=1).

A plot of relative fluorescence against cycle number demonstrates that as few as 10 copies of DNA logic tag T7-76 can be detected (Figure 7). The results were gathered during a real-time PCR experiment using optimized concentrations of reagents, as well as temperature and time settings. In particular, to achieve this sensitivity, it was necessary to measure fluorescence several degrees below the melting temperature of the specific product. This step avoids fluorescence from primer dimers, which may be generated at high cycle numbers in samples with very few or no target sequences. As expected, larger

concentrations of initial DNA logic tag template result in lower cycle threshold (C_t) values. 10^6 copies result in a C_t value of 18.5 cycles ± 0.71 (mean ± s.d.); 100 and 10 copies of DNA logic tags, 100 and 10, have lower C_t values: 20.5 cycles ± 2.12, 21.5 cycles ± 0.71, respectively.

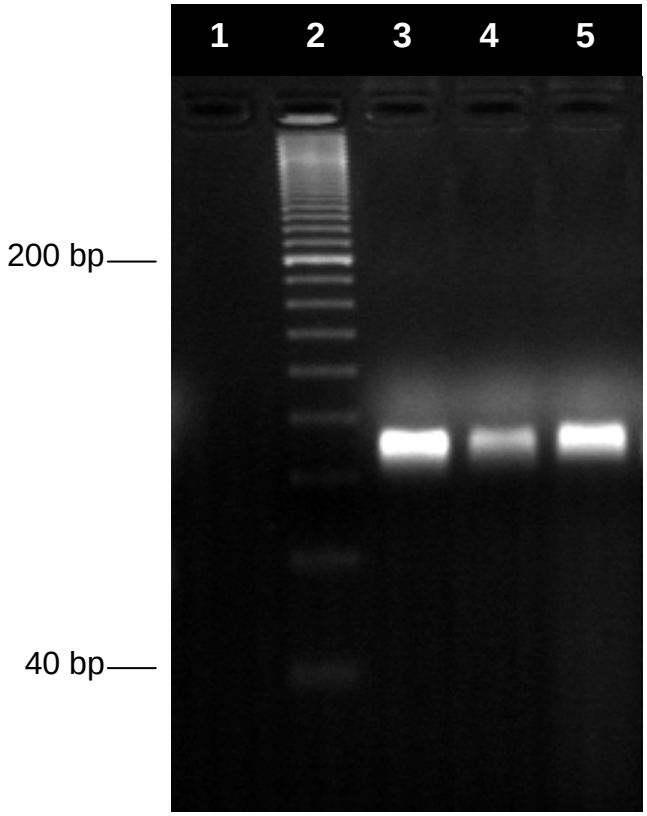

Figure 8. Agarose gel showing products of a typical PCR experiment for a range of template copy numbers. Lane 1: no template (control), Lane 2: DNA ladder, Lane 3: 10^6 copies, Lane 4: 10^2 copies, Lane 5: 10 copies.

The products from the PCR experiment in Figure 7 verified the formation of a single product at the expected product length of 76 base pairs (Figure 8). Samples were

run on a 4% agarose gel at 120 V for 1 hour with SYBR Gold for visualization. Melt curve analysis showed a gradual reduction in fluorescence with increases in temperature. For T7-76, a rapid fall off at 80°C indicated the presence of a specific product that melted at this temperature (data not shown). Once the predicted length of 76 base pairs for T7-76 had been confirmed by agarose gel electrophoresis, melt curve analysis was then used to identify specific products in subsequent analysis. When comparing the product to the ladder, it shows up between 80 base pairs (bp) and 100 bp. This shift of ~20 bp was routinely observed in our gels. This is most likely due to SYBR Gold's interaction with DNA in the ladder, causing the ladder to move slower than other DNA. Also, the increased brightness of 10 copies compared to 100 copies may be due to the use of ROX in the iTaq SYBR Green Supermix as an internal reference dye (bright band in all lanes right above product). Its use may be hindering the level of brightness of the specific product in lane 4.

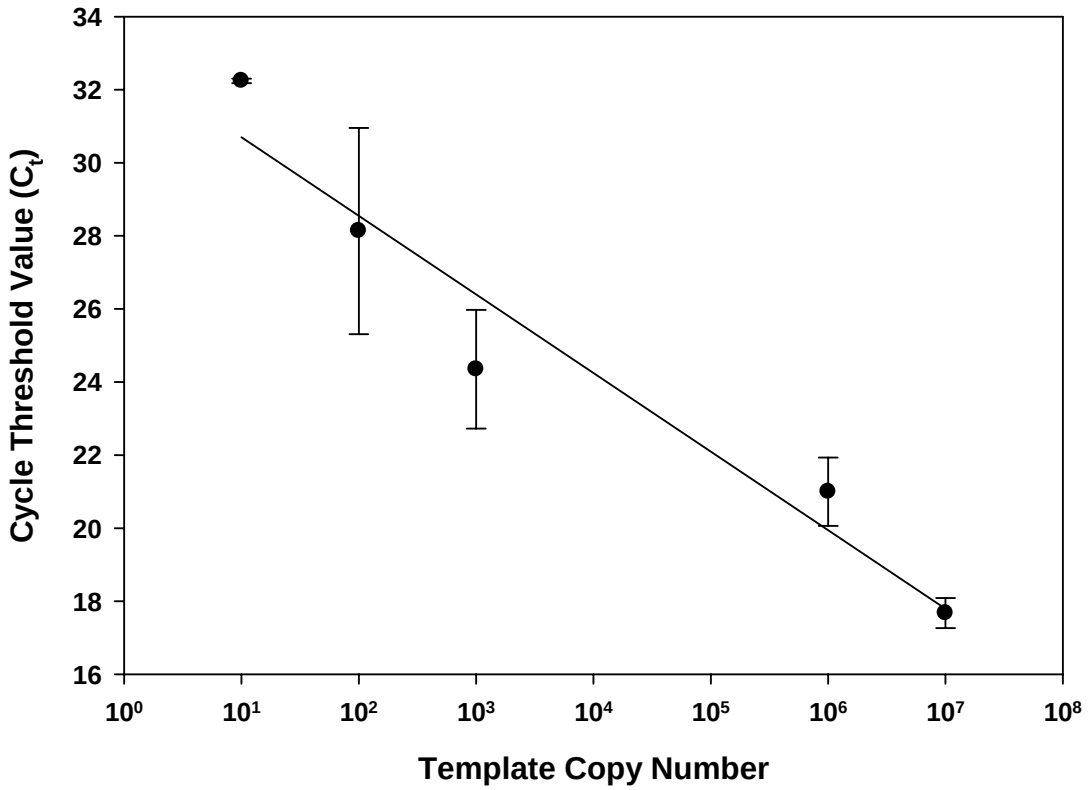

Figure 9. Summary of cycle threshold (C_t) values for a range of initial concentrations of DNA logic tag T7-76. 10 copies: C_t = 32.2 cycles ± 0.1 (mean ± s.d., n = 4); 10^2: C_t = 28.1 cycles ± 2.8 (n = 2); 10^3 copies: C_t = 24.4 ± 1.6 (n=2); 10^6: C_t = 20 cycles ± 1.1 (n = 10), 10^7 copies: C_t = 17.7 ± 0.4 (n=2).

Increasing concentrations of template copy number have decreasing cycle threshold (C_t) values (Figure 9). This graph was generated by combining PCR results from various reactions. Background from each sample was determined by averaging the fluorescence value of the first five cycles; this number was subtracted from all 40 cycles, spanning the entire PCR experiment. C_t values were determined by finding the cycle at which the fluorescence reached 10 units. 100 and 10 copies were consistently amplified.

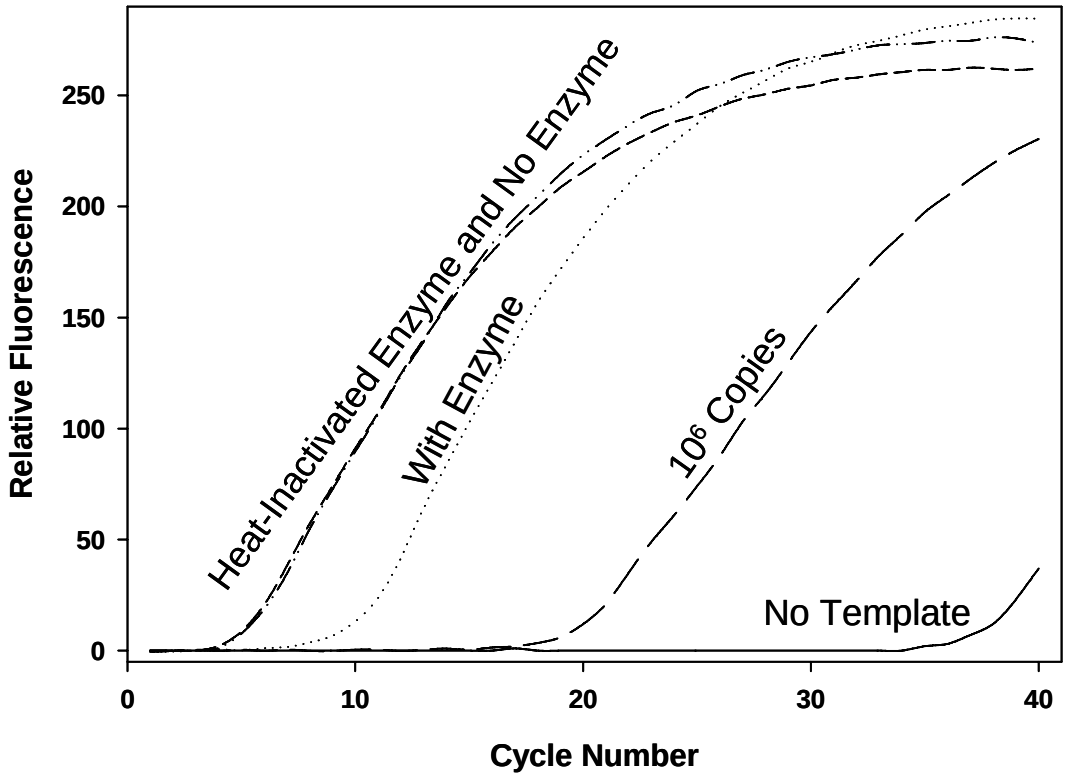

Figure 10. Intact DNA logic tags remaining in solution after restriction enzyme cleavage can be amplified by PCR. C_t values are as follows: Heat-Inactivated and No Enzyme: C_t = 6 cycles ± 1.4 (- - -, mean ± s.d., n=2), With Enzyme: C_t = 10 cycles ± 0.93 (…, n=2); 10^6 copies: C_t = 20 cycles ± 1.1 (- - -, n = 2); No Template: C_t = 38 cycles (—, n = 1).

Enzymatic cleavage of DNA logic tag and its complement reduces the fluorescence and C_t value observed with PCR (Figure 10). This is presumably due to the reduction in template available for PCR amplification. In the heat-inactivated enzyme, no enzyme, and with enzyme reactions, restriction complement DNA logic tag T7-76 and T7_RC-76 was added in a 5:1 ratio, $5x10^{13}$ copies and $1x10^{13}$ copies respectively. This large number of copies was used so results could be visualized using agarose gel electrophoresis (Figure 11). Cleavage of hybridized T7-76 and T7_RC-76 by restriction enzyme HpyCH4V for 1 hour at 37°C results in fewer strands of full-length T7-76, leading to a lower C_t value when amplified. Heat inactivation was successful as the

addition of heat-inactivated enzyme (heated to 95°C for 30 minutes) does not seem to change the C_t value when compared to reactions where the same amount of T7-76 and T7_RC-76 were under the same conditions. Also, addition of buffer supplied with the enzyme does not affect the outcome of PCR (data not shown).

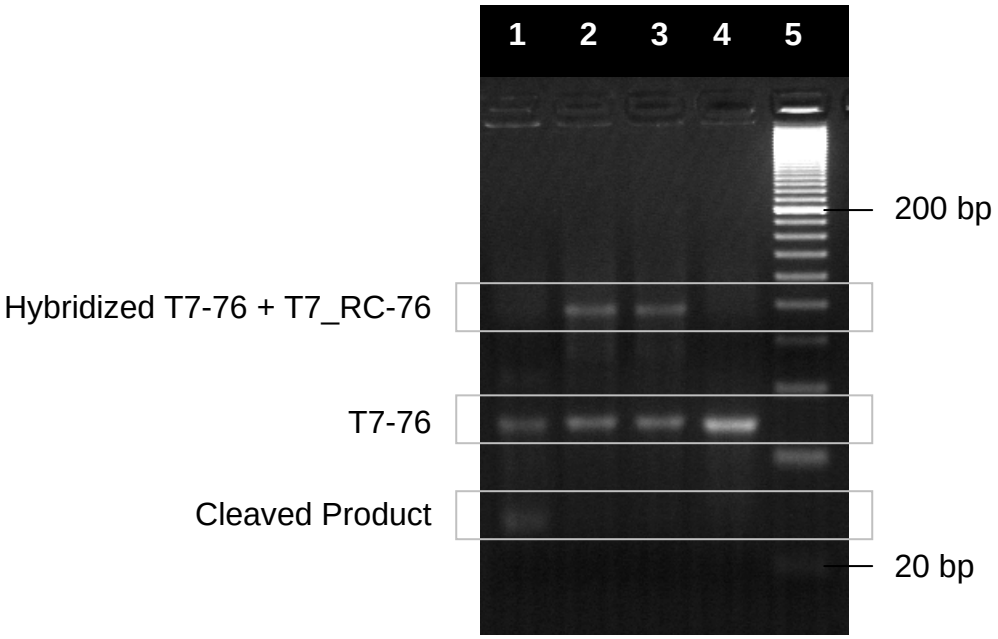

Figure 11. Agarose gel illustrating restriction enzyme cleavage of DNA logic tag T7-76 and its complement T7_RC-76. Lane 1: T7-76 + T7_RC-76 + restriction enzyme (HpyCH4V) + buffers; Lane 2: T7-76 + T7_RC-76 + heat-inactivated HpyCH4V + buffers; Lane 3: T7-76 + T7_RC-76 + buffers (no enzyme); Lane 4: T7-76 alone; Lane 5: DNA ladder. 4% agarose gel stained with SYBR Gold.

Restriction enzyme cleavage of T7-76 and its complement T7_RC-76 results in smaller pieces of DNA when compared to the same concentration of DNA not treated with enzyme (Figure 11). Cleavage only seems to occur in the presence of DNA logic tag T7-76 and its complement (lane 1 vs. lane 3). The agarose gel shows that T7-76 runs as a single band (lane 4). The 20 bp DNA ladder in lane 5 is composed of double-

stranded DNA and, as such, cannot be used to indicate the absolute size of the single-stranded DNA. Adding T7_RC-76 in a 1:5 molar ratio with T7-76 ($1x10^{13}$ copies and $5x10^{13}$ copies respectively) results in a hybridization product that can be cleaved by the restriction enzyme HpyCH4V. There is still a band corresponding to T7-76 since it was added in excess (lane 1). Heat inactivation of HpyCH4V was successful and no cleavage of the hybridization product was observed (lane 2). Further, restriction enzyme digestion is critically dependent on the presence of the tag and its corresponding restriction complement since no digestion was observed without the presence of the complement (lane 4). From the design of T7-76 (Figure 3), we should see a band at 46 bp and 30 bp. While the band at 46 bp is difficult to see, a faint band at 30 bp is visible.

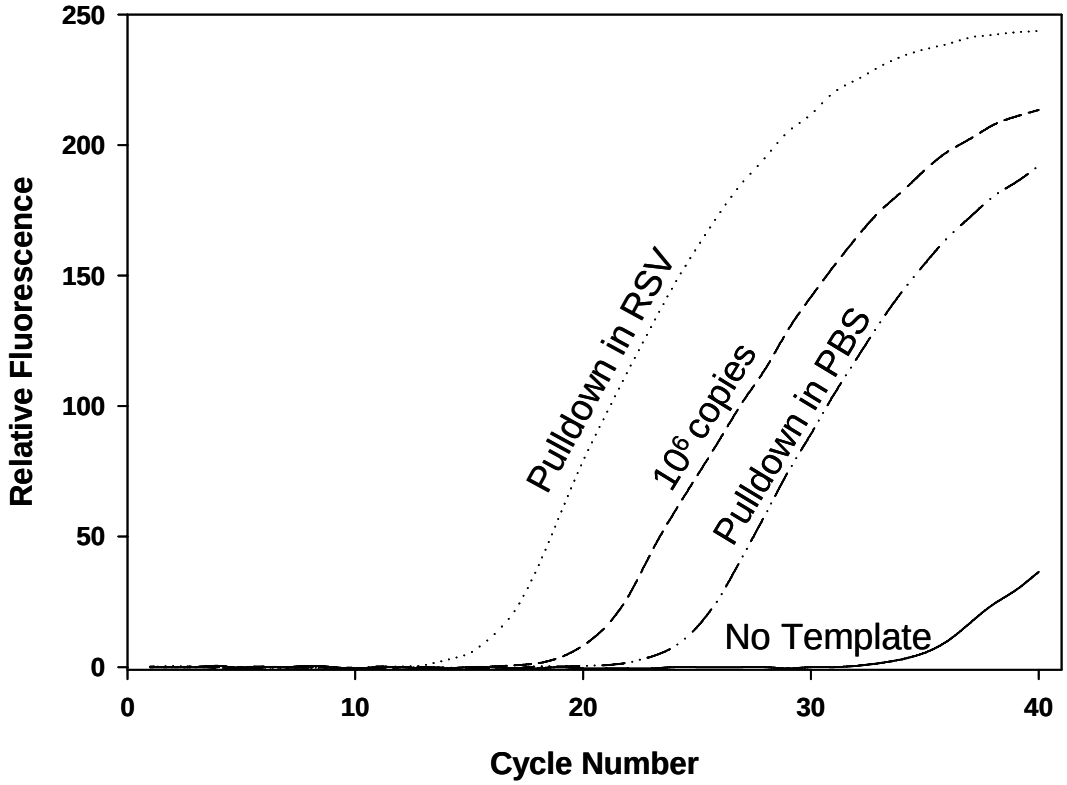

Figure 12. PCR results after magnetic pulldown experiment. Pulldown in RSV (····) had a cycle threshold (C_t) value of 14 (n=4); for 10^6 copies (– – –, positive control for PCR), C_t = 18.75 ± 0.5 (mean ± s.d., n=4), for pulldown in PBS (— ··), C_t = 22.75 ± 1.5 (n=4); for no template (——, negative control), C_t = 35.5 cycles ± 3.54 (n=2).

The presence of RSV delivers DNA logic tags to the analyte solution after a magnetic pulldown experiment (Figure 12). DNA logic tag T7-76 was separated from complementary strands conjugated to gold nanoparticles by applying a magnetic field and heat to a mixture of RSV, magnetic microparticles conjugated to anti-RSV antibodies, and gold nanoparticles conjugated to anti-RSV antibodies and DNA logic tags. The DNA logic tags were then used in a PCR experiment and compared to the amplification of 10^6 copies of T7-76 as a positive control and the same magnetic pulldown run without RSV (in PBS) as a negative control. The pulldown in RSV begins to amplify around 14

cycles, whereas the pulldown in PBS amplifies at around 22.75 cycles. This difference in C_t values implies that there is more T7-76 delivered from the pulldown in RSV than from the pulldown in PBS, suggesting that magnetic microparticles and gold nanoparticles bind RSV and that DNA logic tags are delivered to the analyte solution by magnetic pulldown. The amplification of pulldown in PBS (without RSV) suggests that non-specific binding events also occur which leads to delivery of less, but a significant number of DNA logic tags.

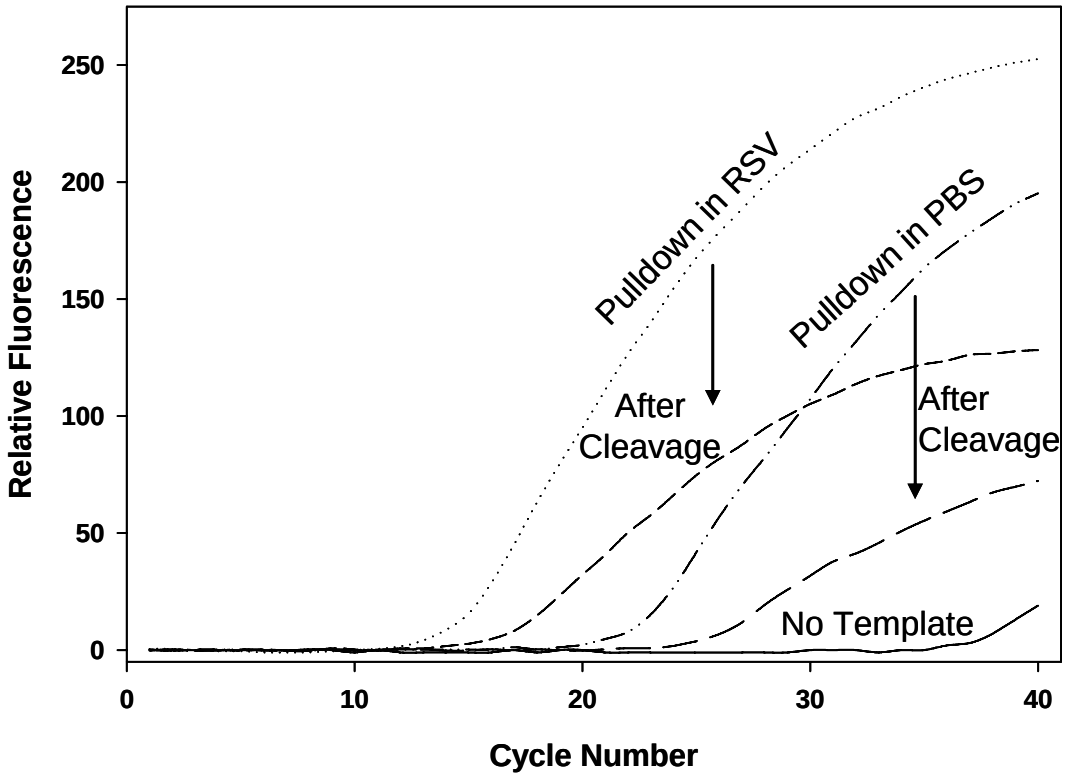

Figure 13. Restriction enzyme cleavage after magnetic pulldown decreases the number of initial template for PCR amplification. For pulldown in RSV, cycle threshold value (C_t) = 12.2 ± 0.12 (mean ± s.d., n = 2); after cleavage, C_t = 14.3 ± 0.42 (n=2). For pulldown in PBS, C_t = 19.8 ± 0.28; after cleavage, C_t = 24 ± 0.57. C_t value for the negative was 36 (n = 1).

Restriction enzyme cleavage on a solution of T7-76 and T7_RC-76 from magnetic pulldown in the presence or absence of RSV decreases the number of templates used for PCR amplification (Figure 13). After magnetic pulldown, the analyte solution was treated with restriction enzyme (HpyCH4V) with buffer and incubated for 1 hour. PCR was run on both the original aliquot from the pulldown and the enzyme-treated solution. From these results, restriction enzyme cleavage has led to a 2-5 increase in C_t value. This is most likely due to a decrease in full-length template for amplification by PCR. Interestingly, the level of fluorescence for the two enzyme-treated aliquots is much lower than that of the original solutions. This may be due to the presence of enzyme and buffer in solution. It may also be the result of primers attaching to primer sites from pieces of DNA from the restriction enzyme cleavage, leading to the amplification of product of less length (Figure 3).

Discussion

The goal of these experiments was to design and evaluate the key components of a new antibody-based detection platform. In preliminary experiments shown in Figure 13, the basic expected outcome was demonstrated: the application of a NOT operation carried out by restriction enzyme cleavage on DNA logic tags led to a lower amount of fluorescence generated by PCR. This result was dependent on experimental validation of each component of the platform's design: coupling of antibody to magnetic microparticles, coupling of antibody to gold nanoparticles, coupling of DNA logic tags and its complementary thiolated sequence to gold nanoparticles, PCR amplification of DNA logic tags, cleavage of DNA logic tag and its restriction complement, and release of

tags from beads. These components supported the approach we set out to explore in Figure 1 and Figure 2.

We examined the effect of coupling F-mix (polyclonal anti-RSV) antibodies to magnetic microparticles in order to verify their functionality. In Figure 4, a mock magnetic pulldown experiment was performed where the gold nanoparticle in our design was replaced with a fluorescent 655 nm quantum dot for visualization. Comparing panel A without conjugated antibodies to panel B with conjugated antibodies, we determined that the antibody was functional and was binding to RSV. Next, we had to ensure that antibodies could retain their functionality when conjugated to gold nanoparticles (Figure 6). By letting antibody-conjugated gold nanoparticles bind RSV on a quartz crystal microbalance, we observed changes in mass over time, presumably due to antibodies on gold nanoparticles binding to virus. To confirm that thiolated sequences complementary to DNA logic tags could also be coupled to gold nanoparticles, we looked at fluorescently labeled DNA strands and compared the amount remaining in supernatant after salt aging with and without gold nanoparticles (Figure 5). Conjugating 70 strands of thiolated DNA complementary to the DNA logic tags allowed us to hybridize around 40 DNA logic tags to each gold nanoparticle (data now shown).

One concern of co-conjugating antibodies and DNA on gold nanoparticles is that if the DNA is too long, it could hinder antibody functionality. Originally, DNA logic tags were smaller, around 40 bp; a thiolated 40-mer DNA strand was to be coupled to gold nanoparticles. As gold nanoparticles and DNA are inherently sticky, the appropriate spacer needed to be added to the thiolated strand to prevent DNA from sitting on the surface of the gold nanoparticle and to provide maximum surface area for antibody

conjugation. Among the four nucleic acids, a 15-mer thymine spacer was used based on literature to provide the necessary barrier between the gold nanoparticles and DNA, increasing the thiolated strand from a 40-mer to a 55-mer.[39] From our initial results, this length did not interfere with antibody conjugation or functionality (QCM tests, similar to Figure 6, data not shown). Due to the constraints on commercial synthesis of DNA, the upper limit for a DNA logic tag was 120 bp. From experiments with 120-mer DNA strands (120 + 15 T-spacer), we determined that antibody functionality was not diminished with DNA of that length (data not shown).

To ensure that our PCR application in itself was sensitive, we tested the lower limits of detection. We were able to amplify 10 copies of DNA logic tags with a significant difference compared to the no template negative control (Figure 7). By running the product on agarose gels, we could also determine that one specific product was being made from various initial template concentrations (Figure 8). This outcome convinced us that DNA logic tags were being amplified when a positive result had a melting temperature of 80°C. Finally, combining the results from different PCR experiments showed consistency in discriminating a range of initial template copy numbers from the no template (negative) control.

A TaqMan probe site was designed for all ten DNA logic tags (Table 1). However, in these initial experiments, the intercalating dye SYBR Green was used instead. Using TaqMan probes would have increased our specificity and decreased our detection of primer dimers. But, using it could have also decreased the amount of fluorescence generated during each amplification cycle. On the other hand, SYBR Green binds to all double-stranded DNA with a preference for G+C regions.[40] These properties

allow for a quick check of any double-stranded product formed during our PCR experiments. Furthermore, purchasing the necessary TaqMan probes for each DNA logic tag designed would have increased our initial costs. Instead, DNA logic tags were decided from SYBR Green experiments. Experiments are underway with the TaqMan probe corresponding to DNA logic tag T7-76 to determine if specificity is increased and what effect, if any, its use has on sensitivity. Also, we will need to determine if the incorporation of uracil instead of thymine will have an impact on the binding of the TaqMan probe.

One discrepancy we noticed during our PCR experiments was that 10-fold changes in initial DNA logic tag concentration did not correspond to a displacement of ~3.3 PCR cycles. This difference is generally seen in PCR experiments because if we assume each cycle doubles the amount of DNA, then $2^{(3.3 \text{ cycles})} = 10$-fold difference.[14] In fact, as seen in Figure 9, starting with 10^2 copies results in a C_t value of 28.1 ± 2.8 (mean ± s.d.); for 10 copies, the C_t value is 32.2 ± 0.1. A 10-fold lower concentration led to a 4-cycle difference. This could be due to the settings of the reaction or the type of DNA polymerase used. We will need to ascertain the efficiency of our polymerase by running further tests to improve the reactions and to optimize the difference in C_t values among varying concentrations of starting template.

Another problem we found was that our product did not line up with the correct molecular weight on the DNA ladder; this 20 bp shift between ladder and product was observed with all DNA logic tags and with different lots of ladder from the same manufacturer (Figure 8 and Figure 11). To remedy this, we will first test other stains. Ethidium bromide is generally used to stain gels; however, due to its increased toxicity

and lower sensitivity, it was not used in this application. But, it is possible that it would not have as great of an effect on DNA migration as SYBR Gold. Also, post-staining the gel instead of adding the stain directly to the DNA could solve this problem because the dye would not affect DNA migration. We will also explore using ladders from different manufacturers.

Next, we determined that restriction enzyme cleavage by the enzyme HpyCH4V led to degradation of T7-76 and its complement. First, we had carefully designed logic tag T7-76 and T7_RC-76 to contain a site for restriction enzyme digestion (Figure 3, Table 1). We first ran agarose gels with large amounts of logic tag and its complement to observe degraded product (Figure 11). Next, we ran PCR on lower concentrations of product to find that there was a decrease in the amount of usable templates when HpyCH4V was first applied (Figure 10).

Finally, we demonstrated that the solution phase complex of magnetic microparticles conjugated to antibodies and gold nanoparticles conjugated to antibodies and DNA logic tags can be used to bind virus and deliver DNA logic tags to an analyte solution. When PCR was performed after a virus pulldown, DNA logic tags could be amplified (Figure 12). Furthermore, there was a significant difference between the amounts of DNA logic tags that were amplified from a virus pulldown versus a pulldown that did not contain virus (in PBS). The PCR results also showed that non-specific binding or the generation of false positives is inherent within this antibody-based detection strategy. When the magnetic pulldown was performed in PBS alone, template was still delivered, most likely due to unbound gold nanoparticles remaining in solution during separation and washing steps. This solution contained DNA logic tag T7-76 and

amplified well above the negative control that contained no template (Figure 12). If we had not seen this result, non-specific binding would probably still occur when the pulldown is run in cell lysate. We could verify this by running a magnetic pulldown with non-specific antibody and then running PCR on the output with primers designed for T7_RC-76; if amplification does occur, it would be due to non-specific binding.

One aspect of DNA logic tag delivery is how to release the logic tags from the magnetic pulldown. In the current design, thiolated strands are conjugated to the gold nanoparticle with DNA logic tags hybridized directly to them. They are then released by heating. Another method for releasing DNA logic tags is to directly conjugate them to the gold nanoparticles and then release them using DTT. This difference may lead to an increased number of DNA logic tags associated to each gold nanoparticle and, in turn, to each virus or pathogen. However, there could also be a negative effect of DTT on the efficiency of the following restriction enzyme and PCR experiments. Another aspect of DNA logic tag delivery is the possibility that subsequent PCR processes may amplify a part of the cell lysate. When designing logic tags for a specific detection application, a BLAST search should also be done against the genome of the pathogen of interest.

These preliminary results suggest that this is a feasible and promising application to reduce the number of DNA logic tags that result from non-specific antibody binding. Certain factors remain to be studied, for example, the optimal parameters for the restriction enzyme cleavage reaction as well as the limits of sensitivity and specificity of the NOT operation. Experiments to examine these aspects are underway.

CHAPTER III

FUTURE DIRECTIONS

Although the research described here deals with the detection of a specific test virus (RSV), we believe similar results will be seen with other viruses and molecular structures that can be selectively bound by antibodies.

Within this present application, parameters of restriction enzyme cleavage, such as incubation times and enzyme concentration, after magnetic pulldown still need to be optimized. Also, various limits remain to be tested. First, the limits of restriction cleavage need to be explored. In particular, we would like to know at what concentration of DNA logic tags associated to non-specific binding events do cleavage reactions become ineffective. Also, we would like to examine the constraints of the system by looking at how low and high concentrations of virus affect the outcome. Finally, we would like to test the upper and lower limits of sensitivity and specificity of our application.

We would also like to explore the use of other logical operations AND and OR. The AND operation may be beneficial in decreasing the presence of false positives by requiring two or more binding events to occur in order to produce a signal. Two different DNA logic tags and two different monoclonal antibodies would be coupled to gold nanoparticles. Similar to the NOT operation, the different tags will be delivered to an analyte solution. Next, ligation templates or small pieces of DNA complementary to the ends of the tags will be added. After they hybridize, DNA ligase will be used to ligate

the ends of the logic tags, creating one large strand of DNA. During PCR, primers specific to only this large strand would be added. Any signal would be the result of amplification of the ligated DNA strand and would be associated with two specific binding events, increasing the certainty of the output by decreasing the rate of false positives.

The logical OR operation is another application of this general design. For the OR operation, different tags associated with different antibodies coupled to gold nanoparticles will be delivered to an analyte solution. During PCR, primers to all of these logic tags will be added as well as the corresponding TaqMan probes with different fluorophores, which will allow for analysis of different tags in parallel. This approach could especially be important in detection of molecular markers in diseases like cancer where there is an interplay between which markers are present and in what concentrations.

Another manipulation of this design is to conjugate DNA strands instead of antibodies onto the gold nanoparticles to create a detection method for patterns of biomarkers. These DNA strands could be complementary to DNA and RNA. By associating DNA logic tags with DNA, RNA, and proteins, another molecular patterning strategy can be implemented to see if all three are present in solution (AND) and if there are any differences in concentration among the different biomarkers (OR).

Additionally, we would like to add a quantitative approach to all of these operations which would allow us to describe the amount of antigen present in solution by only looking at the results of PCR. Furthermore, we would like to produce mathematical relationships to describe the results of these operations. For example, for the NOT

reaction, we could form relationships that describe the use of specific and non-specific antibodies in comparison to using specific antibodies alone.

A variety of detection techniques could benefit from this design, everything from the detection of virus to biomarker patterns to biological threat agents. We believe that this strategy utilizes well-established molecular biology techniques using DNA as inputs to logical operations in order to increase accuracy, precision, sensitivity, and specificity of detection applications.

REFERENCES

1. Voller, A., Bartlett, A. & Bidwell, D. E. Enzyme immunoassays with special reference to ELISA techniques. J Clin Pathol 31, 507-20 (1978).

2. Sano, T., Smith, C. L. & Cantor, C. R. Immuno-PCR: very sensitive antigen detection by means of specific antibody-DNA conjugates. Science 258, 120-2 (1992).

3. Nam, J. M., Thaxton, C. S. & Mirkin, C. A. Nanoparticle-based bio-bar codes for the ultrasensitive detection of proteins. Science 301, 1884-6 (2003).

4. Pillai, S. D. Rapid molecular detection of microbial pathogens: breakthroughs and challenges. Arch Virol Suppl 13, 67-82 (1997).

5. Feng, P. Impact of molecular biology on the detection of foodborne pathogens. Mol Biotechnol 7, 267-78 (1997).

6. Iqbal, S. S. et al. A review of molecular recognition technologies for detection of biological threat agents. Biosens Bioelectron 15, 549-78 (2000).

7. van der Zee, H. & Huis in't Veld, J. H. Rapid and alternative screening methods for microbiological analysis. J AOAC Int 80, 934-40 (1997).

8. Prusiner, S. B. Prions. Proc Natl Acad Sci U S A 95, 13363-83 (1998).

9. Iqbal, S. S., Chambers, J. P., Brubaker, R. R., Goode, M. T. & Valdes, J. J. Detection of Yersinia pestis using branched DNA. Mol Cell Probes 13, 315-20 (1999).

10. Chernoff, D. N. et al. Quantification of cytomegalovirus DNA in peripheral blood leukocytes by a branched-DNA signal amplification assay. J Clin Microbiol 35, 2740-4 (1997).

11. Saiki, R. K. et al. Primer-directed enzymatic amplification of DNA with a thermostable DNA polymerase. Science 239, 487-91 (1988).

12. Mullis, K. B. The unusual origin of the polymerase chain reaction. Sci Am 262, 56-61, 64-5 (1990).

13. Heid, C. A., Stevens, J., Livak, K. J. & Williams, P. M. Real time quantitative PCR. Genome Res 6, 986-94 (1996).

14. Bustin, S. A. A-Z of quantitative PCR (International University Line, La Jolla, CA, 2004).

15. Landegren, U., Kaiser, R., Sanders, J. & Hood, L. A ligase-mediated gene detection technique. Science 241, 1077-80 (1988).

16. Kohler, G. & Milstein, C. Continuous cultures of fused cells secreting antibody of predefined specificity. Nature 256, 495-7 (1975).

17. Niemeyer, C. M., Adler, M. & Wacker, R. Immuno-PCR: high sensitivity detection of proteins by nucleic acid amplification. Trends Biotechnol 23, 208-16 (2005).

18. Mirkin, C. A., Letsinger, R. L., Mucic, R. C. & Storhoff, J. J. A DNA-based method for rationally assembling nanoparticles into macroscopic materials. Nature 382, 607-9 (1996).

19. Thaxton, C. S., Hill, H. D., Georganopoulou, D. G., Stoeva, S. I. & Mirkin, C. A. A bio-bar-code assay based upon dithiothreitol-induced oligonucleotide release. Anal Chem 77, 8174-8 (2005).

20. Cheng, M. M. et al. Nanotechnologies for biomolecular detection and medical diagnostics. Curr Opin Chem Biol 10, 11-9 (2006).

21. Mason, J. T., Xu, L., Sheng, Z. M. & O'Leary, T. J. A liposome-PCR assay for the ultrasensitive detection of biological toxins. Nat Biotechnol 24, 555-7 (2006).

22. Gullberg, M. et al. Cytokine detection by antibody-based proximity ligation. Proc Natl Acad Sci U S A 101, 8420-4 (2004).

23. Gullberg, M. et al. A sense of closeness: protein detection by proximity ligation. Curr Opin Biotechnol 14, 82-6 (2003).

24. Fredriksson, S. et al. Protein detection using proximity-dependent DNA ligation assays. Nat Biotechnol 20, 473-7 (2002).

25. Stone, G. P., Mernaugh, R. & Haselton, F. R. Virus detection using filament-coupled antibodies. Biotechnol Bioeng 91, 699-706 (2005).

26. Nettikadan, S. R., Johnson, J. C., Mosher, C. & Henderson, E. Virus particle detection by solid phase immunocapture and atomic force microscopy. Biochem Biophys Res Commun 311, 540-5 (2003).

27. Bentzen, E., Wright, D. W. & Crowe Jr, J. E. Nanoscale tools for rapid and sensitive diagnosis of viruses. Future Virology 1, 769-781 (2006).

28. Chen, R. J. et al. An investigation of the mechanisms of electronic sensing of protein adsorption on carbon nanotube devices. J Am Chem Soc 126, 1563-8 (2004).

29. Perez, J. M., Simeone, F. J., Saeki, Y., Josephson, L. & Weissleder, R. Viral-induced self-assembly of magnetic nanoparticles allows the detection of viral particles in biological media. J Am Chem Soc 125, 10192-3 (2003).

30. Wu, X. et al. Immunofluorescent labeling of cancer marker Her2 and other cellular targets with semiconductor quantum dots. Nat Biotechnol 21, 41-6 (2003).

31. Bentzen, E. L., House, F., Utley, T. J., Crowe, J. E., Jr. & Wright, D. W. Progression of respiratory syncytial virus infection monitored by fluorescent quantum dot probes. Nano Lett 5, 591-5 (2005).

32. Ruben, A. J. & Landweber, L. F. The past, present and future of molecular computing. Nat Rev Mol Cell Biol 1, 69-72 (2000).

33. Adleman, L. M. Molecular computation of solutions to combinatorial problems. Science 266, 1021-4 (1994).

34. Bath, J. & Turberfield, A. J. DNA nanomachines. Nature Nanotechnology 2, 275-284 (2007).

35. Kolpashchikov, D. M. & Stojanovic, M. N. Boolean control of aptamer binding states. J Am Chem Soc 127, 11348-51 (2005).

36. Stojanovic, M. N. et al. Deoxyribozyme-based ligase logic gates and their initial circuits. J Am Chem Soc 127, 6914-5 (2005).

37. Seelig, G., Soloveichik, D., Zhang, D. Y. & Winfree, E. Enzyme-free nucleic acid logic circuits. Science 314, 1585-8 (2006).

38. Simpson, D. A., Feeney, S., Boyle, C. & Stitt, A. W. Retinal VEGF mRNA measured by SYBR green I fluorescence: A versatile approach to quantitative PCR. Mol Vis 6, 178-83 (2000).

39. Storhoff, J. J., Elghanian, R., Mirkin, C. A. & Letsinger, R. L. Sequence-Dependent Stability of DNA-Modified Gold Nanoparticles. Langmuir 18, 6666-6670 (2002).

40. Giglio, S., Monis, P. T. & Saint, C. P. Demonstration of preferential binding of SYBR Green I to specific DNA fragments in real-time multiplex PCR. Nucleic Acids Res 31, e136 (2003).